Interactive comment on "Plant functional diversity affects climate–vegetation interaction" *by* V.P. Groner et al.

V.P. Groner et al.

27 February 2018

Author's response

We thank the referees very much for comments and suggestions, and we address the main issues arising out of the comments in the corresponding responses. Based on the comments by referees and the editor, we made some major changes in the manuscript (among others):

1. We included a more detailed description of plant diversity during the AHP in the introduction to account for the comment by Referee #1 (page 1, line 18ff).

2. We extended the description of competition in JSBACH as well as the description of the experimental set up including an extension of Tab. 1 by albedo and roughness length, and limitations accompanying our assumptions mainly due to the choice of SST/SIC.

3. We rephrased parts of the manuscript that were not clear to the referees, for example about the standard PFT set in JSBACH (page 3, line 30), grass establishment after fire (page 8, line 26), the data processing for Fig. 5 (page 9, line 23ff), the potential of rate of vegetation cover and precipitation decline (page 10, line 26), the use of the term dominant branch" (page 10, line 32), and we elaborated more on alternative approaches to the PFT concept (page 12, line 12ff).

4. We included exact latitudes and longitudes for the study domain as well as the regions that are discussed in more detail.

Interactive comment on "Plant functional diversity affects climate–vegetation interaction" *by* V.P. Groner et al.

V.P. Groner et al.

27 February 2018

Response to Anonymous Referee #1 – Received and published: 22 December 2017

"The manuscript submitted by Groner et al to "Climate of the Past" discusses the influence of variations in plant functional types on climate at the end of the Holocene. The article is nicely written. However, it is based on assumptions that should be more fully argued or explained."

In order to consider your comment, we have to check back here if you actually refer to Groner et al. (2015) published in Climate of the Past, or if the first part of your comment concerns the present manuscript, submitted to Biogeosciences. For now we assume that you refer to the present manuscript.

"It has been shown for many years (actually, since the palaeogeographic map drawn up by N. Petit Maire et al., UNESCO-IGCP 252, 1993 and more recently through the reconstructions performed by e.g. Hély and Lézine, 2014) that plant cover in the Sahara during the Holocene was primarily not homogeneous with co-occurrence of plants that are today found in distinct phytogeographical areas. Desert plants are typically found in the Sahara today. These plants co-occurred during the late Holocene with tropical trees probably in restricted areas such as river or lake banks. Actually, pollen data show that tropical trees were present but we are unable to infer any evaluation of their coverage in the landscape from pollen data. In other words, palynologists show that the Holocene increased rainfall led to a dramatic increase in biodiversity. There has been no replacement of one biome by another but rather an interpenetration of plants taxa that are found today in distinct biomes. Moreover, the vegetation cover had a mosaic-like character and was certainly discontinuous."

We fully agree with your summary of the vegetation distribution during the African Humid Period. We based our study mainly on Hély et al. (2014) and their description of a highly diverse mosaic-like vegetation cover during the African Humid Period, see page 1 line 18. We agree that special features such as gallery forests must be described in more detail and we gladly introduce an additional descriptive paragraph to the introduction.

"An quantified evaluation of the vegetation cover would certainly be possible by applying the algorithms developed by Sugita and colleagues (2007) in West Africa."

As mentioned at the end of the introduction (page 2, line 29-31), "With our idealized set up, we do not expect our simulations to match reconstructions, rather we focus on qualitative differences between simulations to find mechanisms relevant for the question how PFT diversity affects climate–vegetation interaction."

"The importance of the coverage of one biome with respect to another one seems to me an important parameter to take into account, particularly if tropical trees were mostly restricted to the edges of streams and lakes. One of the major characteristics of plant distributions in dry areas is the presence of gallery forests along rivers or open

water surfaces. These gallery forests can host tropical trees far from the climatic zone they originate from. In this case, trees are not in equilibrium with climate and survive under drier conditions only thanks to available ground waters. Actually we do not know since when the water available in the soil is no longer able to compensate for the lack of precipitation."

As mentioned above, we agree that gallery forests should be mentioned in the introduction as they are a crucial part of the study. EXPTD10 with the additional frost-tolerant tropical tree PFT aims at representing gallery forest, not spatially but conceptually. We understand that further description is necessary here and we gladly adjust the manuscript to make it more clear.

"In this context, could you please precise what are the 21 PFTs used in your study, based on the plant types identifyed in pollen studies carried out in the Sahara and Sahel and how do you evaluate the coverage and distribution of each of them for the time periods you have selected."

JSBACH provides 21 PFTs but we used only 8 in this study, summarized in Tab. 1. The cover fraction of each PFT is calculated by the model as a result of climatic conditions and competition as described in the manuscript Section 2.1.

"Additional comments:

(1) Temperature of the coldest month: To my knowledge, tropical climates are characterized by relatively constant (hot) temperature throughout the year and a large diurnal amplitude. One of the most important factors for plant distributions is rainfall and the length of the dry season, not temperature (at least in the lowlands). This, of course, in the case of a "climatic" and not an azonal distribution as is the case of forest galleries"

We agree on that, however during the mid-Holocene winter temperatures were cooler in North Africa than today, and our model simulated temperatures below the bioclimatic threshold, thus tropical trees could not establish in the experiments. With the experiment EXPTD10 we introduce the aspect of favourable microclimatic conditions especially in gallery forests.

"(2) C3/C4 grasses: roughly 30% of the Poaceae growing in the Sahara today are C3, particularly those growing in wet places and in the highlands (Maire Monod, 1950; Quézel, 1965; Maire, 1952; Quézel Santa, 1962; Quézel, 1954; Gillet, 1968....)".

The vegetation distribution presented in this study is a result of model simulations. We observe the occurrence of C3 grasses especially in the Mediterranean and in highlands, however under the given boundary conditions, C4 grasses are in our model more productive than C3 and thus the dominant grass PFT in most of the study domain.

Interactive comment on "Plant functional diversity affects climate–vegetation interaction" *by* V.P. Groner et al.

V.P. Groner et al.

27 February 2018

Response to Anonymous Referee #2 – Received and published: 26 January 2018

This manuscript aims to assess the sensitivity of the simulated extent of green Sahara during the African Humid Period (AHP), and the manner in which the land cover from this green Sahara transitions to current desert conditions, to the representation of plant functional types (PFTs) in the MPI-ESM (i.e. the PFT diversity). The subject of the manuscript is of broad interest and many past studies have addressed the question of the extent of green Sahara. Authors claim that differences in past studies are due to representation of different PFTs in different models (this appears to be a valid argument based on results presented in this manuscript) but the general strength of the land-atmosphere feedbacks (which depends on a particular land surface model) likely also plays a role. That is, the extent of green Sahara will be different amongst models despite same PFTs because different land surface models have different strengths of land atmosphere coupling. In addition, different land surface models will likely represent same PFTs with different parameterizations and parameter values. This aspect is not discussed in the manuscript.

The strength of land atmosphere coupling surely plays an crucial role for the extent of the green Sahara and has been considered in previous modelling studies, see references page 2, line 1. The new contribution to the question of the extent of the green Sahara in the present study is the explicit consideration of plant functional diversity – which has so far not been considered in models of higher complexity than the conceptual models by Claussen et al. (2013) and Groner et al. (2015) – at the example of JSBACH.

We do not claim that the representation of PFTs is the most and only important factor determining the extent of the green Sahara, though we illustrate that the choice of PFTs can have a significant impact on the climate-vegetation system. The representation of PFTs as well as the strength of land atmosphere coupling differ of course between models, but we expect that the observed effects are qualitatively not limited to JSBACH and might also apply to other models. A complete evaluation of effects on climate-vegetation interaction and the comparison between different land surface models goes beyond the scope of this study.

This study can be assessed in the context of paleo vegetation as the first reviewer appears to have done but also in the context of land-atmosphere interactions which is where my expertise lies. In my opinion, the manuscript needs clarification of several items before it may be considered for publication in BG.

The competition between PFTs is an important aspect of this study but I felt that the description on page 4 (lines 5 – 25) wasn't sufficient for me as a reader to understand how competition actually works. Since this is a modelling study, I feel it is important to lay it out for the reader. The text on page 5 attempts to do this but it seems it doesn't go all the way.

As the model we used in this study was described in detail in previous publications, see eg. Brovkin et al. (2009), Reick et al. (2013), we confined ourselves to providing an brief overview over the most important aspects of competition in JSBACH. Based on your comment, we understand that further description is necessary here and we gladly adjust the manuscript to make it more comprehensible for the reader.

Other comments

Having read the authors' response to Reviewer #1 I now realize out of 21 PFTs only 8 PFTs can grow in the region considered. However, when I read the manuscript the first time I had similar confusion. So perhaps this point needs to be clarified.

We understand that the phrasing is confusing here and we gladly adjust the manuscript to make it more clear.

Section 2.2 needs more info about model setup and discussion of implications of how this set up is done.
1) How does use of present day SSTs affects the overall results? Does an interactive ocean generally amplify or dampen the effect of land-atmosphere feedbacks?

It has been shown that the west African monsoon and the seasonal cooling of the equatorial Atlantic amplify each other, see e.g. Okumura et al. (2004). Thus, the use of present day SST probably reduces the overall strength of the west African monsoon in mid-Holocene simulations. Thereby the simulated precipitation and vegetation cover fractions are probably lower than with AHP SST. We would expect an interactive ocean to generally amplify the monsoon signals caused by changes in PFT composition.

Our study focuses on the effect of plant functional diversity rather than synergies that might occur with an interactive ocean. As we prescribed SST identically for all simulations, we do not expect qualitative differences in the results. Nevertheless, we gladly add this information to the manuscript.

2) Other atmospheric boundary conditions correspond to what time period?

Other atmospheric boundary conditions are prescribed after IPCC AR5 (2013). Tropspheric methane is by default prescribed with a constant mixing ration of 1.69 ppmv. N_2O is by default prescribed with a constant mixing ration of 309 ppbv. CFC11 and CFC12 are prescribed with constant mixing ratios of 0.253 ppbv and 0.466 ppbv, respectively. Other CFC species are currently not included. The default ozone climatology is given as three-dimensional monthly values, although in the stratosphere, ozone is assumed to not vary with longitude, and is based on the merged and future ozone climatology as described by Cionni et al. (2011) for CMIP5. The stratospheric aerosol is based on an extension of the Pinatubo aerosol data set (Stenchikov et al., 1998) to cover the entire period between 1850 and 1999. We will add this information to the manuscript.

3) What do soil properties mean – do you mean soil texture and permeable soil depth.

By soil properties we refer here mainly to the soil depth until the bedrock and the water holding capacity. These properties are generated from a compilation of data sets, provided as input maps to the model (Hagemann et al., 2014). Further parameters and their references are summarized in Hagemann et al. (2014). For our study it is most relevant that in the 5-layer scheme soil scheme in JSBACH (Hagemann et al., 2014) the number of active layers is limited by the depth until the bed rock. Thus, the soil water content may be greater than 0 only for those layers with a soil depth above the bedrock as there is no water available for the land surface scheme within the bedrock. Soils in the present day Sahara are very shallow compared to the mid-Holocene, especially in mountainous regions, and have a very low water holding capacity making growth difficult for PFTs with high moisture requirements even though provided precipitation is sufficient.

Accounting for the changes in soil properties during the AHP would probably further amplify the feedback between land surface and atmosphere. However, as mentioned above, we focus here on the effects of plant functional diversity. Nevertheless, we gladly add more information about soil properties to the manuscript.

4) Since land-atmosphere feedbacks are key to understanding the results presented in this manuscript it would be useful to put albedo, typical LAI, rooting depth and vegetation height of different PFTs in a table for reader to understand how the different physical characteristics of a PFT can potentially affect land-atmosphere interactions.

We gladly extend the table by albedo values for the considered PFTs. The maximum LAIs listed in Tab. 1 can be assumed as typical LAIs for the presented PFTs since the LAI quickly increases to that value in an asymptotic way as soon as growth conditions are favourable in terms of moisture availability, bioclimatic limits and growing season. The rooting depth is assumed to be the same for all PFTs following the rooting depth map provided by Hagemann et al. (2014). We will add a description to manuscript. JSBACH has no explicit implementation of vegetation height, it is implicitly considered through the roughness length, a parameter we can easily attach to the table for clarification.

On Page 6, around line 24, it is mentioned albedo in the C4 grass simulation is lower than that in the EXP_{ALL} simulation. Is this an error? Grasses are generally brighter than trees. But then on page 7, lines 11 and 12, the manuscript correctly notes that albedo is higher in EXP_{C4} than in EXP_{ALL}. Please correct the sentences on page 6 so that they are consistent with the text on page 7.

The manuscript is correct here, we consider different regions in the two examples you mentioned. In the first example, we describe the effects in region 1, where grasses are darker compared to the bare soil that prevails in EXP_{ALL}. The second example refers to region 2 where grasses are brighter compared to the trees that prevail in EXP_{ALL}. We agree that the formulation is not clear and we gladly adjust the manuscript to highlight the difference.

On Page 7, line 2, the phrase "slows down water and energy fluxes" is unclear. What does slowing down means does it mean decrease in fluxes. If yes, which fluxes – I suppose evapotranspiration (i.e. latent heat). Please be explicit.

By slowing down we mean here that the absolute fluxes decrease, including sensible and latent heat flux, evapotranspiration and precipitation. We will adjust the formulation for clarification.

Page 7, line 16-20. Yes, C4 grasses are more productive than C3 grasses. But productivity is different than specific leaf area (SLA, m2/kg C) which is a measure of how many m2 of leaves can be constructed with a Kg of carbon of leaf biomass. The discussion in lines 16-20 appears to be mixing productivity with SLA.

We agree that the formulation is not explicit here, we will adjust the formulation for clarification.

Page 7, line 21. "Grass cover is not directly reduces by disturbances". This seems contradictory to what happens in nature. Grasses are more flammable than trees so fires affect grass cover more drastically – although, of course, grasses spring back faster too.

We understand your confusion here and we agree with your argumentation. Grasses are of course affected by fire, they burn in JSBACH just like other PFTs. What we wanted to express here is that the cover fraction of grasses does not change if fire occurs because grasses automatically establish on uncolonized land in the following year. We will adjust the formulation for clarification.

Page 7, line 33. "...SRG outcompetes C4 due to the implicit assumption of light competition". So are shrubs assumed to be taller than trees. This is where a more complete description of how competition works can help. A model can simulate the actual physical processes or it can assume that certain hierarchy in vegetation superiority exists. It seems in this case, the model assumes that shrubs are always superior to grasses and

if they can exist then they will take over grasses. Is this correct? Is this a reasonable assumption.

We agree that a more detailed description of the competition is necessary to follow our argumentation here. The model assumes a hierarchy in vegetation superiority. Shrubs belong to the class of woody PFTs and are therefore always superior to grasses, among other things because they are assumed to be taller, see roughness length. We assume this to be an ecologically reasonable assumption.

The purpose of additional description of the competition module is to highlight all primary assumptions and structure of the competition module while acknowledging its limitations. Yes, models aren't perfect but if their features and limitations are well highlighted then it's easier for readers to put the results in the context of the model.

We agree that mentioning the limitations of a model is just as important as the description of its features, thus we gladly include a brief summary in the manuscript. In terms of vegetation dynamics, one important limitation is surely the representation of plant diversity with a static set of discrete PFT parameters which does not cover the range of species categorized as one PFT and disregards phenotypic plasticity and trait variability which are often larger within PFTs than between PFTs (see page 10, line 27-29). Additionally, the fauna which plays an important role in savannas in terms of grazing is not represented in JSBACH, and nutrient availability which is a limiting factor of plant growth is not considered.

Page8, Section 3.2, lines 15-16. "...we subtract 100-year averages of consecutive time slices..." only becomes clear once a reader looks at Figure 5. Please reword this sentence to make it more clear.

We will reword this sentence for clarification as follows "For a first estimate of regional transition patterns from the "green" Sahara (8 ky) to the "desert" state (0 ky), we calculate differences between consecutive time slices (8 ky-6 ky, 6 ky-4 ky, 4 ky-2 ky, 2 ky-0 ky) of the 100-year averages of P and veg_{max} for all simulations, and compare the resulting transition maps of P and veg_{max} in the whole study domain (12 to 34° N, -15 to 40° E).".

In Figure 5 the units of precipitation change make sense. The units of precipitation are mm/year and then the change is mm/year per 2k year. This can be simplified and referred to change in annual precipitation and then the units would just be mm/2k years. However, the units of change in fractional vegetation cover seem incorrect. What does fraction/year (i.e. year^(-1)) means? Why is there a year in the denominator? If change in fractional cover over 2k years is being referred to then units should just be fraction/2k years. I am unclear why there's an additional year^(-1) term needed.

We choose these units because the change in each 100-year averaged value is mm/yr for precipitation and fraction/yr for vegetation cover fraction and we want to represent the difference between two consecutive time slices, thus in 2000 years. The change is not mm/2000yr but mm/yr over 2000 years. The same accounts for vegetation cover fraction with the change in fraction/yr in 2000 years.

Page 9, line 4. It took me a while to realize that $delta_P$ and $delta_{veg_{max}}$ do not refer to zonal averages but instead Figure 6 shows zonal averages of these quantities. Please consider rewording this sentence.

We will reword this sentence for clarification as follows "For the quantitative comparison of all simulations, we condense the information of the transition maps by calculating zonal means (-15 to 40° E) of P and veg_{max} and subtracting consecutive time slices. These zonally averaged differences between consecutive time slices are in the following referred to as ΔP and Δveg_{max}."

Page 9, lines 14-16. I wasn't able to follow this sentence.

With this sentence we want to describe that the initial values of vegetation cover fraction and precipitation contribute to the potential rate of decline. If the initial values are low, there is no potential to show a decrease a large as starting from a higher value. We will rephrase this part for clarification.

Page 9, line 21. What is a "dominant branch"?

The dominant branch refers to the curve most of the points lie on in contrast to the outlying data points. We understand that this formulation is confusion, we will rephrase the sentences including that formulation.

Page 10, towards the end of section 3.2, it is discussed how disappearance of SRG leads C4 grasses to establish and an increase in fractional vegetation cover for same precipitation. 1) Why does SRG disappears, and 2) isn't this behaviour (of higher fractional vegetation cover for same precipitation) unrealistic.

SRG disappears because the environmental conditions are no longer supporting its growth, in particular precipitation is too low. The increase in vegetation cover fraction of C4 can be explained by the lack of competition from SRG. All available water can be used by C4 and as it has a lower SLA, it is able to cover a larger area with less precipitation. That is an ecologically reasonable behavior.

Page 10, line 9. "...with a strong feedback between single plant types and climate". This sentence is unclear.

We will reword this sentence as follows "Our findings thereby reconcile a gradual transition from a "green" state to a "desert" state with a strong feedback between vegetation and climate."

On page 10, and earlier on, does "realized PFTs" means the PFT that can potentially exist in a grid cell.

As described on page 5, line 32-33, we refer to the "potential" PFT diversity as the number of PFTs allowed in a simulation and to the "realized" PFT diversity as the number of PFTs that actually establish in a grid cell.

Page 10, last two sentences. Please explain "trait flexibility" and "evolutionary optimality hypothesis" in one or two sentences.

We will reword this part as follows "Alternative approaches to represent plant diversity consider the simulation of individual plants (e.g. LPJ-GUESS (Smith et al., 2001); aDGVM (Scheiter et al., 2013), "trail variability" which allows selected traits to vary within the range of observations to optimize growth under the environmental conditions (e.g. JSBACH (Verheijen et al., 2013,2015), "trait flexibility" which represents plant diversity in terms of plant ecophysiological trade-offs instead of PFTs by selecting for the most suitable growth strategy out of randomly generated sets of parameter values (e.g. JeDi-DGVM (Pavlick, 2012); aDGVM Scheiter et al., 2013)), or operate based on the "evolutionary optimality hypothesis", an approach based on the microeconomic standard framework to determine the optimal input mix for a two-input production process, here water loss and carbon gain during photosynthesis (Wang et al., 2017). "

In context of issue raised by Reviewer #1 also consider showing absolute annual temperatures for 8k years ago and temperature change relative to 0k to justify the need for tropical tree PFT that can survive 10 degree Celsius coldest month temperature.

Although winter temperatures were on average lower at 8 ky than at 0 ky, the affected region (around 18 to 22 deg N) is slightly warmer at 8 ky in our simulations. However, the minimum temperature of the coldest month for tropical trees falls below the threshold of 15.5 deg Celsius at 8k as well as 0 ky. The difference is that at 8 ky, precipitation is substantially higher than at 0 ky which allows tropical trees to sustain growth as soon as established. Therefore, we did not to include a figure of temperature differences in the manuscript, but we agree that an additional explanation in Sec. 2.3 will serve clarification.

Figure 4 is an important figure. Figure 5 is also an important figure which illustrates whether the change in precipitation and fractional vegetation cover is gradual or immediate. However, overall as a reader I felt that this discussion wasn't enough or complete to convey the primary message around how the system operates. Perhaps, a simple cartoon of Figure 4 can be used to help understand a reader the discussion around Figure 4 e.g. using horizontal and vertical lines touching the Y and the X axes, respectively.

We understand that the interpretation of Fig. 4 might be difficult without further illustration of the thresholds we discuss in the text. We gladly include supporting lines in the graphs to make it easier to capture the differences between the experiments.

I am also attaching an annotated version of the manuscript with my hand written comments a lot of which I have already summarized here. But please see this version for other minor comments.

We will consider your comments in the revision of the manuscript, thank you very much for the careful evaluations.

Plant functional diversity affects climate–vegetation interaction

Vivienne P. Groner[1,2], Thomas Raddatz[1], Christian H. Reick[1], and Martin Claussen[1,3]

[1]Max Planck Institute for Meteorology, Bundesstraße 53, 20146 Hamburg, Germany
[2]International Max Planck Research School on Earth System Modelling, Bundesstraße 53, 20146 Hamburg, Germany
[3]Center for Earth system research and Sustainability, Universität Hamburg, Bundesstraße 53, 20146 Hamburg, Germany

Correspondence to: V. P. Groner (vivienne.groner@mpimet.mpg.de)

Abstract.

We present how variations in plant functional diversity affect climate–vegetation interaction towards the end of the African Humid Period (AHP) in coupled land-atmosphere simulations using the Max Planck Institute Earth System Model MPI-ESM. In experiments with AHP boundary conditions, the extent of the "green" Sahara varies considerably with changes in plant functional diversity. Differences in vegetation cover extent and Plant Functional Type (PFT) composition translate into significantly different land surface parameters, water cycling and surface energy budget. These changes have not only regional consequences but considerably alter large scale atmospheric circulation patterns and the position of the tropical rain belt. Towards the end of the AHP, simulations with the standard PFT set in MPI-ESM depict a gradual decrease of precipitation and vegetation cover over time, while simulations with modified PFT composition show either a sharp decline of both variables or an even slower retreat. Thus, not the quantitative but the qualitative PFT composition determines climate–vegetation interaction and the climate–vegetation system response to external forcing. The sensitivity of simulated system states to changes in PFT composition raises the question how realistically Earth system models can actually represent climate–vegetation interaction, considering the poor representation of plant diversity in the current generation of land surface models.

1 Introduction

The "African Humid Period" (AHP) is an exceptionally interesting period to study drastic climate and vegetation changes in the past. During this period around 11,700 to 4,200 years ago, rainfall was substantially higher than today across much of West and North Africa (Bartlein et al., 2011; Shanahan et al., 2015) ~~,~~ and rivers and lakes were widespread (Hoelzmann et al., 1998; Kröpelin et al., 2008; Lézine et al., 2011a; Drake et al., 2011)~~, and~~. Pollen records indicate that the Sahel boundary was shifted northward by 5 to 7° to at least 23° N (Jolly et al., 1998) and tropical plant taxa might have used river banks as migration paths to enter drier environments forming gallery forests (Watrin et al., 2009). Consequently, vegetation cover marked a diverse savanna-like mosaic of xeric and tropical species ~~covered large areas of the nowadays hyperarid Sahara and arid Sahel region (Watrin et al., 2009; Hély et al., 2014).~~ whose ranges do not overlap today (Hély et al., 2014).

The establishment of this so-called "green" Sahara (Ritchie and Haynes, 1987; Jolly et al., 1998) was presumably triggered by changes in the Earth's orbit resulting in a stronger insolation and higher temperatures in the boreal summer than today, accompanied by an intensification and northward shifted West African monsoon (Kutzbach, 1981; Kutzbach and Guetter, 1986). It has been shown that these externally triggered changes were amplified by internal feedback mechanisms involving ocean (Kutzbach and Liu, 1997; Braconnot et al., 1999; Liu et al., 2004), surface water coverage by lakes and wetlands (Coe and Bonan, 1997; Krinner et al., 2012), dust (Pausata et al., 2016; Egerer et al., 2016), soil albedo (Knorr and Schnitzler, 2006; Vamborg et al., 2011), and vegetation (Claussen and Gayler, 1997; Texier et al., 1997; Doherty et al., 2000; Rachmayani et al., 2015). However, despite increasing understanding of these involved feedbacks, the extent of the "green" Sahara substantially differed between previous modelling studies and all models underestimated the northward extent reconstructed from palaeo proxy data (see Claussen et al., 2017).

Similar to the establishment of the "green" Sahara, there is scientific consensus that the desertification of the southern Sahara and Sahel region towards the end of the AHP was triggered by a gradual decline in incoming solar radiation due to changes in the Earth's orbit which caused a weakening and southward shift of the West African monsoon. ~~Conversely~~However, the timing and abruptness of the transition from the "green" Sahara to the "desert" state are as yet uncertain, among other things because the ~~relevance~~ role of climate–vegetation ~~feedback~~ feedbacks in this context is still under debate. Under the assumption of a strong positive climate–vegetation feedback, ~~multiple~~ at least two stable equilibria could exist for the Sahara region – a "green" state with high vegetation cover and a "desert" state without vegetation (Claussen, 1994; Claussen and Gayler, 1997; Brovkin et al., 1998; Bathiany et al., 2012) ~~– and the potential~~ The non-linearity of this feedback ~~might~~ can potentially cause an abrupt transition between these states when the system reaches a "tipping point" (Williams et al., 2011). While some studies indicated such an abrupt collapse of vegetation towards the end of the AHP implying a strong climate–vegetation feedback (Claussen et al., 1999; deMenocal et al., 2000), others suggested a more gradual decline of vegetation (Kröpelin et al., 2008; Lézine, 2009; Lézine et al., 2011b) and precipitation (Francus et al., 2013) or attributed the collapse to other triggers (Liu et al., 2007; Rachmayani et al., 2015) thereby questioning the ~~existence of a strong~~ strength of climate–vegetation ~~feedback~~feedbacks.

Based on a conceptual modelling study, Claussen et al. (2013) proposed that these different viewpoints are not contradicting if one accounts for plant diversity. High plant diversity in terms of moisture requirements could stabilize a climate–vegetation system by buffering strong feedbacks between individual plant types and precipitation, whereas a reduction in plant diversity might allow for an abrupt regime shift under gradually changing environmental conditions. Hence, climate–vegetation feedback strength would not be a ~~universal~~ unique property of a certain region but also depend on ~~the~~ its vegetation composition. An ecological assessment of the conceptual approach by Claussen et al. (2013) and an adjustment of their model to AHP plant types corroborated their results (Groner et al., 2015). These findings raise the question how the representation of plant functional diversity influences climate–vegetation interaction in models of higher complexity and thereby affects the extent of the "green" Sahara as well as the timing and rate of the transition to the "desert" state. To our knowledge, no previous comprehensive modelling study on the AHP has explicitly considered the effect of plant functional diversity on climate–vegetation interaction. To close this gap, we present here a series of coupled land-atmosphere simulations from mid-Holocene to preindustrial with different combinations of Plant Functional Types (PFTs) using the Max Planck Institute Earth System Model MPI-ESM. With our idealized set up, we do not expect our simulations to match reconstructions, rather we focus on qualitative differences between simulations to find mechanisms relevant for the ~~question how PFT diversity affects~~ role of PFT diversity in climate–vegetation ~~interaction~~interactions.

2 Model set up

2.1 MPI-ESM

We use for our study the Max Planck Institute Earth System Model MPI-ESM, a comprehensive Earth system model that couples model components for the atmosphere (ECHAM6, Stevens et al. (2013)), ocean (MPIOM, Jungclaus et al. (2013)) and land surface (JSBACH, Raddatz et al. (2007); Reick et al. (2013)) through the exchange of energy, momentum, water and carbon dioxide. This study focuses on the coupling between the atmospheric component and the land surface component.

ECHAM6 is an atmospheric General Circulation Model (GCM) which was developed at the Max Planck Institute for Meteorology in Hamburg, Germany. The model focuses on the coupling between diabatic processes and large-scale circulations which are both driven by solar insolation. For each time step the model determines the large-scale horizontal circulation with a spectral hydrostatic dynamical core. Additionally, other physical processes (turbulent diffusion, convection, clouds, precipitation, gravity wave drag, diabatic heating by radiation) are calculated for each vertical column of the Gaussian grid associated with the truncation used in the spectral dynamical core. These processes are coupled with the horizontal circulation each time step by transforming the variables that represent the atmospheric state from the spectral representation to the Gaussian grid and back. However, radiative transfer is computed extensively only once per hour for solar radiation (14 bands) as well as terrestrial radiation (16 bands).

As integral component of ECHAM6, JSBACH provides the lower atmospheric boundary conditions over land ~~as well as~~ and simulates both biogeochemical and biogeophysical ~~degrees of freedom that arise from~~ terrestrial processes. JSBACH simulates land-surface properties interactively in terms of soil moisture, snow cover, leaf area index, and vegetation distribution. Plant diversity is represented in JSBACH in discrete functional plant classes, so-called “Plant Functional Types” (PFTs). The ~~standard JSBACH set provides 21 PFTs representing natural vegetation, crops and pasture. The~~ submodel for biogeographic vegetation shifts accounts for ~~only~~ 8 PFTs, shown in Tab. 1. Natural land cover change and vegetation dynamics are simulated in JSBACH by the DYNVEG component ~~(Brovkin et al., 2009)~~ based on a number of principles commonly used in Dynamic Global Vegetation Models (DGVMs), briefly summarized ~~in the following. For a detailed description see Reick et al. (2013)~~here, followed by a description of the implementation in JSBACH. For more details see Brovkin et al. (2009); Reick et al. (2013).

The “universal presence principle” implies that each PFT can potentially grow everywhere (“seeds are everywhere”). Physiological constraints define the climatic range within which a certain PFT can exist. Such bioclimatic limits only prohibit establishment if conditions are not suitable for a PFT to grow, but do not prevent further existence when values fall out of this range. The increase or reduction ~~of land~~ in fractional vegetation cover is determined by two processes. ~~First~~The first possibility for land cover to increase or decrease is that inhospitable regions can expand or shrink. This change in area available for growth affects the cover of all PFTs. Second, PFT cover can be reduced by natural death or disturbance (e.g. wildfires) and increased by migration into space opened in this way, so-called “uncolonized land”. The different PFTs compete for this uncolonized land while vegetation establishment is generally only possible when net primary productivity (NPP) is positive at least for some years. Competition is considered in DYNVEG by a hierarchy in vegetation superiority based on growth form and ~~by productivity. After disturbances, grass PFTs have an advantage because they quickly migrate in the new space while woody~~

~~PFTs~~ NPP. Woody PFTs (trees and shrubs) ~~regrow slowly. The tree-grass ratio depends on the rate of disturbances. Within~~ are assumed to be dominant over grass PFTs by reason of light competition; within the woody PFTs, competition is regulated by productivity: higher NPP means a competitive advantage ~~.~~ because PFTs with higher NPP migrate faster into uncolonized land. ~~In absence of disturbance, woody PFTs are dominant over grass PFTs by reason of light competition. The second possibility for land cover to increase or decrease is that inhospitable regions can expand or shrink. This change in area available for growth affects the cover of all PFTs~~If uncolonized land is available, grass PFTs have a competitive advantage because they quickly migrate in the new space while woody PFTs regrow slowly. However, grasses can establish only on uncolonized land, whereas trees and shrubs establish also on already vegetated land. So, in the absence of disturbances, grasses are gradually superseded by woody vegetation and the tree-grass ratio eventually depends on the rate of disturbances.

The dynamic modelling of natural vegetation is based on fractions of unit area in a grid cell as the state variables in DYNVEG. A composition of woody (w_i), grass (g_i), and uncolonized (u) cover fractions compose the whole area within a grid cell where vegetation ~~cannot~~ can grow (veg_{max}):

$$u + \sum_{i=1}^{N^w} w_i + \sum_{i=1}^{N^g} g_i = 1 \; , \tag{1}$$

where N^w and N^g are the number of woody and grass PFTs, respectively.

The dynamics of ~~the~~ woody and grass PFT cover fractions are governed by ~~the~~ a coupled set of differential equations that account for establishment, natural mortality, and ~~disturbances~~ disturbance-driven mortality (fire, wind throw)~~, acting on characteristic timescales~~ :

$$\frac{dw_i}{dt} = \frac{\theta(u) w_i}{\tau_i^{(w)}} \frac{\overline{NPP}_i^{\alpha}}{\sum_{n\epsilon W} w_n \overline{NPP}_n^{\alpha}} - \frac{w_i}{\gamma_i^{(w)}} - w_i D^w(\boldsymbol{w},\boldsymbol{g}) \; , \tag{2}$$

$$\frac{dg_j}{dt} = \frac{u g_j}{\tau_j^{(g)}} \frac{\overline{NPP}_j}{\sum_{n\epsilon G} g_n \overline{NPP}_n} - \frac{g_i}{\gamma_i^{(g)}} - g_j D^g(\boldsymbol{w},\boldsymbol{g}) \; . \tag{3}$$

The establishment of a woody PFT i, represented by the first term on the right hand side in Eq. 2, depends on its cover fraction fraction w_i, its characteristic establishment time scale $\tau_i^{(w)}$, and its competitive strength in terms of long-term average NPP ($\overline{NPP}_i$, in mol(C) m^{-2} s^{-1}) compared to other woody PFTs. The exponent α is set to 1.5 to control the competition between woody PFTs by suppressing the establishment with small NPP. The step function θ accounts for the area available for establishment which is one for $u > 0$ and otherwise zero. The establishment of grass PFTs (first term on the right hand side in Eq. 3) is similar to woody establishment except for the assumption that grass can establish only within the area left available after tree establishment. This ensures the competitive advantage of woody PFTs over grasses in the absence of disturbances such as fires.

Natural mortality, represented by the second term on the right hand side in Eq. 2, 3, is assumed to be proportional to the abundance of the particular vegetation type and acts on a characteristic timescales $\gamma_i^{(w)}$ / $\gamma_i^{(g)}$ for woody and ~~for grass types (see Reick et al., 2013).~~ grass PFTs, respectively. Due to the lack of knowledge, it is assumed that τ_i=γ_i, see Tab. 1.

Disturbance-driven mortality, represented by the third term on the right hand side in Eq. 2, 3, accounts for mortality due to fire and wind throw. For wildfires to happen in JSBACH, sufficient above ground plant litter has to be available for combustion, and the litter needs to be sufficiently dry, meaning below a threshold, to catch fire. Fire disturbance rate is assumed to increase linearly with decreasing humidity, and depends on the extent of woody and grass PFTs via the value of the above ground litter. Wind disturbance accounts for the reduction in forest cover by storms which is of minor importance in our study. For a description of the disturbance equations see Reick et al. (2013).

The result is the potential natural vegetation cover in a world without humans. DYNVEG also includes a sophisticated approach to account for a human aspect, but we do not consider anthropogenic land cover change here.

The dynamics of the fraction of inhospitable land ($d = 1 - veg_{max}$) in a grid cell are calculated in DYNVEG with a separate submodel in order to determine the extent of cool deserts like the Arctic region or hot deserts like the Sahara. The extent of d determines the fraction of a grid cell where vegetation ~~can~~ cannot grow. The model is based on the idea that deserts develop when the long term NPP average drops below a threshold so that vegetation cannot ~~establish~~ build a canopy at least once a year. The fraction ~~f~~ veg_{max} of a model grid cell with substantial vegetation cover at least once in year (y) is

$$\underline{f}veg_{max}(y) = \sum_{i \in W} w_i (1 - e^{-a(LAI_i^{max})^b}) + \sum_{i \in G} g_i \frac{g+u}{g} (1 - e^{-a(LAI_i^{max})^b}) \,, \tag{4}$$

where $g = \sum_{i \epsilon G} g_i$ is the total grass fraction of vegetation, and LAI_i^{max} is the maximum leaf area that appeared during the year y. LAI_i^{max} is determined from the maximum biomass in leaves by

$$LAI_i^{max}(y) = SLA_i \cdot C_{G,i}^{max}/3 \,, \tag{5}$$

where $C_{G,i}^{max}$ is the maximum living biomass found in PFT i in the considered year. One third of the biomass is assumed to be in the leaves, and the specific leaf area (SLA_i) relates the carbon content of leaves to their area. The parameter $a = 1.95$ is chosen such that the simulated distribution of hot and cold deserts matches observations. The parameter $b = 2$ describes steepness of the transition between vegetation and desert and has been chosen to give a realistic distribution of deserts. Since one year of low growth does not make a desert, we assume a delayed response to changes in growth conditions where the time scale for desert development is chosen as 50 years.

2.2 Set up of simulations

We perform global coupled land-atmosphere simulations with a horizontal resolution of approximately 1.88° (T63) and 47 vertical levels. The model runs with dynamic vegetation for the periods 8 ky (ky = 1000 years before present), 6 ky, 4 ky, 2 ky, and 0 ky for 300 years with the first 200 years corresponding to a spin up period to reach a state close to equilibrium; the first 100 years of the spin up period run with three times accelerated vegetation dynamics. In the standard JSBACH configuration, the seasonal canopy albedo is calculated as a function of leaf area index, whereas the bare soil albedo is a grid box constant derived from satellite measurements (see Otto et al., 2011). To account for darker soils below vegetation, we implement for the study domain (~~12~~11.19 to ~~34~~33.57° N, ~~-15 to 40~~15.94° W to 40.31° E, see Fig. 1) a simple albedo-scheme that reduces the soil albedo according to the mean net primary productivity of the preceding five years (based on Vamborg et al. (2011)). Soil

~~properties~~ types originate from the FAO digital soil map of the world (FAO/UNESCO, 1974)~~. Due to lack~~, soil characteristics such as soil depth, soil porosity, and soil field capacity are prescribed after Hagemann and Stacke (2015). In the absence of palaeo soil data, we are obliged to assume that the soil characteristics during the AHP were the same as they are today. To attain equilibrium states, we set orbital parameters (Berger, 1978) and CO_2 concentrations (Joos, 2016) to fixed values for each time slice experiment, see Tab. 2. Other atmospheric boundary conditions (trace gas concentrations, stratospheric ozone, aerosol distribution, spectral solar irradiance, orography) remain unchanged ~~over time~~at representative present-day values (Stevens et al., 2013). Moreover, we prescribe sea ice concentration (SIC) and sea surface temperatures (SST) identically for all simulations using data from Hurrell et al. (2008) in cyclical repetition (1945 to 1974). The use of present day SST probably reduces the overall strength of the west African monsoon in mid-Holocene simulations as it has been shown that the west African monsoon and the seasonal cooling of the equatorial Atlantic amplify each other, see e.g. (Okumura and Xie, 2004). Thereby the simulated precipitation and vegetation cover fractions are probably lower than with AHP SST. The consideration of an interactive ocean would probably further amplify the monsoon signals caused by changes in PFT composition. However, as mentioned above, we do not expect our simulations to match reconstructions and our study focuses on the effect of plant functional diversity rather than synergies that might occur with an interactive ocean. As we prescribed SST identically for all simulations, we do not expect qualitative differences in the results.

2.3 Modifications of plant functional diversity

To investigate the effects of changes in plant functional diversity on climate–vegetation interaction towards the end of the AHP, we perform four different types of simulations: as a baseline serves the simulation EXP_{ALL} with all natural PFTs commonly used in JSBACH (Tab. 1). The second type of simulation is a single-PFT experiment EXP_{C4} which features only C4 Grass ($C4$) and thereby excludes all woody PFTs and their competition in the study domain. Third, we combine the woody PFTs Tropical Evergreen Tree (TE) and Raingreen Shrub (SRG) with C4 Grass in the study domain for the experiments $EXP_{TE,C4}$ and $EXP_{SRG,C4}$. The ~~forth~~ fourth type of simulation addresses the representation of bioclimatic limits in JSBACH. During the ~~experimental phase of the~~ present study, we found that the minimum temperatures of the coldest month fall in some regions in north Africa below the bioclimatic limit of Tropical Evergreen and Deciduous Trees (15.5°C) and thereby prevent their establishment in areas where reconstructions indicate the presence of tropical trees during the AHP (Hély et al., 2014). Although the definition of this limit is based on an empirical relationship between mean temperatures of the coldest month and absolute minimum temperature (frost occurrence) (Müller, 1982; Prentice et al., 1992), favorable microclimatic conditions could have allowed tropical taxa to establish, especially in gallery forests. Another argument is that there might have been taxa that were partially frost tolerant and could survive short periods of freezing temperatures. A literature-based compilation of experimental cold tolerance thresholds for leaves (evergreens), buds and twigs or stem illustrates that "tropical evergreens show damage at - 1°C or -2°C. Many of the broad-leaved evergreens can tolerate - 10 to -15°C, with a few able to survive -20°C" (Harrison et al., 2010). In order to test the model sensitivity to this limit, we add a newly designed tropical frost tolerant woody PFT (TD_{10}) with relaxed bioclimatic limits to the standard PFT set in EXP_{TD10}. The minimum temperature of the coldest month is for TD_{10} reduced from 15.5 to 10°C, while all other parameters ~~equate to the~~ remain the same as for the Tropical

Deciduous Tree PFT (TD), see Tab. 1. In all simulations, the initial cover fractions are equally distributed over all included PFTs in the study domain.

In the following, we refer to the "potential" PFT diversity as the number of PFTs allowed in a simulation and to the "realized" PFT diversity as the number of PFTs that actually establish in a grid cell. We present the effects of changes in plant functional diversity on 1) climate–vegetation interaction during the AHP and the extent of the "green" Sahara (8 ky), and on 2) the timing and rate of the transition from the "green" Sahara to the desert state.

3 Results

3.1 Effects on climate–vegetation interaction during the AHP

Changes in plant functional diversity significantly affect climate–vegetation interaction and the extent of the "green" Sahara under AHP boundary conditions (8 ky). Figure 2 illustrates precipitation (P) and vegetation cover fraction (veg_{max}) for the experiment with the standard PFT set (EXP_{ALL}) as well as differences between EXP_{ALL} and simulations with modified PFT composition. Already at the first glance, it becomes apparent that P and veg_{max} considerably differ between experiments: EXP_{C4}, $EXP_{TE,C4}$, and EXP_{TD10} depict in most of the study domain a "greening" associated with higher P compared to EXP_{ALL} (Fig. 2c-f, i-j) while $EXP_{SRG,C4}$ shows a "browing" and less P (Fig. 2g, h).

A closer look reveals substantial regional differences within each simulation. To identify the underlying causes, we compare land surface parameters, energy surface budget, and hydrological cycle in the two most affected regions (see Fig. 2): the transition zone between desert and savanna (Region 1: ~~18~~18.65 to ~~22~~22.38° N, ~~5~~4.69 to ~~30~~30.94° E) and the region southwest of the transition zone (Region 2: ~~12~~11.19 to ~~18~~18.65° N, ~~-15 to 20~~15.94° W to 19.69° E). Tab. 3 summarizes selected ~~parameters~~ variables averaged over the last 100 simulated years in the two regions for EXP_{ALL} as well as differences to the other simulations. The fractions (f_i) of PFTs with a substantial contribution to the total vegetation cover fraction veg_{max} are shown in Tab. 4. Further, we consider how changes in land surface parameters, surface energy balance, and hydrological cycle translate into alterations of large scale circulation features associated with the West African monsoon focusing on the lower-level Inner Tropical Convergence Zone (ITCZ, 925 hPa), the mid-level African Easterly Jet (AEJ, 600 hPa), and the upper-level Tropical Easterly Jet (TEJ, 150 hPa) during the monsoon season (June to September) (Fig. 3). The term "ITCZ" is ambiguous since literature provides very different definitions based on wind convergence, surface air pressure and rainfall or outgoing longwave radiation. Hereinafter, we refer to the ITCZ as the surface feature over the African continent that marks the convergence of northeasterly Harmattan winds that originate in the Sahara and the southwest monsoon flow that emanates from the Atlantic, also named Inner Tropical Front.

In Region 1 in EXP_{C4}, $EXP_{TE,C4}$, and EXP_{TD10}, the lower albedo due to higher veg_{max} compared to EXP_{ALL} enhances the absorption of solar energy available for evapotranspiration which heats the lower atmosphere, accelerates energy and water cycling, and boosts moisture available in the atmosphere. This does not only increase the likelihood for regional convective precipitation, but also enhances the meridional temperature and moisture gradient between the equator and the northern Tropics. This gradient is a good indicator of how far north the monsoon flow penetrates into Africa (Bonfils et al., 2001). The increase of this gradient results in a northward shift of the ITCZ, a weakening and northward shift of the AEJ, a strengthening of the TEJ, and consequently, a northward shift of the tropical rain belt (Fig. 3c-f, i-j). These changes are in accordance with literature: wetter than average conditions in the Sahel are linked to a weaker and northward shifted AEJ (Nicholson and Grist, 2003; Nicholson, 2013) and a stronger TEJ (Grist and Nicholson, 2001; Jenkins et al., 2005; Nicholson, 2008; Hulme and Tosdevin, 1989).

~~Complementary~~Conversely, the higher albedo in $EXP_{SRG,C4}$ compared to EXP_{ALL} lowers the absorption of solar energy available for evapotranspiration which ~~slows down~~ decreases water and surface energy fluxes, dries and cools the atmosphere, and suppresses precipitation in Region 1. The resulting reduction in the meridional atmospheric moisture and temperature gradient causes a southward shift of the ITCZ, the AEJ and the core of the rain belt (Fig. 3g, h). In agreement with literature, a more equatorward position of the AEJ is associated with drier than average conditions over the Sahel (Nicholson and Grist, 2003; Nicholson, 2013). However, the weakening of these two tropical jets is usually linked to wet conditions which is not the case in $EXP_{SRG,C4}$. This could be attributed to the low water recycling efficiency of vegetation compared to EXP_{ALL}, especially due to SRG, which implies less release of latent heat in the atmosphere which in turn decreases convection (Texier et al., 2000).

In Region 2 in EXP_{C4} and $EXP_{TE,C4}$, and EXP_{TD10}, veg_{max} varies only little with changes in PFT composition compared to EXP_{ALL}, but P is largely affected by the physical properties of prevailing PFTs. In EXP_{C4}, the high grass albedo, compared to tropical tree PFTs that ~~covers~~ cover a substantial fraction of Region 2 in EXP_{ALL} (Tab. 4), reduces the absorption of incoming solar radiation and surface energy fluxes. Additionally, the limited evapotranspiration capacity of the $C4$ PFT due to a comparatively small maximum leaf area ($LAI_{max,i}$) limits the transfer of interception and soil water to the atmosphere (Tab. 1). Together with the small surface roughness of $C4$, which reduces turbulent fluxes, this decreases the likelihood of precipitation south of the tropical rain belt (Fig. 3c). Based on the assumption that less precipitation supports less plant growth, one would expect both veg_{max} and P to be lower in EXP_{C4} than in EXP_{ALL}. However, the efficient growth of $C4$ compensates the lower P relative to EXP_{ALL}. $C4$ requires less water to cover the same area with leaves than other PFTs (Fig. 4b) because $C4$ has a high SLA_i, a high NPP (Tab. 1), and the photosynthetic C4 pathway enables a high water use efficiency. For example, to cover 1 m^2 area with 1 m^2 leaves, $C4$ needs around 210% less ~~NPP~~ carbon than TE and around 260 % less than SRG (derived from Eq. (4),(5)). Additionally, ~~grass cover is not directly reduced by disturbances~~grasses re-establish within one year after fire disturbance.

The moderate effects on precipitation in $EXP_{TE,C4}$ reflect the relatively small changes in land surface properties because the PFT composition is almost identical to EXP_{ALL} (Tab. 4). In EXP_{TD10}, the increase in P in Region 2 results mainly from a lower albedo, a higher surface roughness, and a higher evapotranspiration in Region 1 as well as in the northwestern part of the study domain due to a higher contribution of tree PFTs which limits SRG growth. This strongly enhances the West African monsoon (Fig. 3i,j) and thereby significantly increases rainfall over large areas of the study domain. Such an albedo induced enhancement of precipitation in the Sahel region has been shown in previous MPI-ESM experiments (Bathiany et al., 2010; Vamborg et al., 2011).

In $EXP_{SRG,C4}$, veg_{max} is in Region 2 lower than in the other simulations with the same precipitation (see Fig. 2e, f, 4d). The explanation lies in the parameterisation of SRG and in the implementation of competition in JSBACH. Due to a low SLA_i (Tab. 1), SRG requires a higher NPP to cover the same area with leaves as another PFT. SRG's comparatively low photosynthetic capacity and low $LAI_{max,i}$ however impedes reaching a NPP in the order of magnitude as other PFTs (Fig. 4d). When competition is calculated in JSBACH, SRG outcompetes $C4$ due to the implicit assumption of light competition (see Sect. 2.1). Since growth conditions are not optimal for SRG in the study domain facing water competition with $C4$ – all PFTs use water from the same soil water reservoir – SRG cannot fill the pools of living biomass over the growing season, which leads to an expansion of desert area (see Eq. (4), (5)). SRG thereby acts as a desert promoter in JSBACH. Complementary, the lack of SRG in EXP_{C4} and $EXP_{TE,C4}$ reduces the competitive pressure on TE and $C4$ and their higher growth efficiency facilitates their expansion and the repression of desert. The desert promoting effect of shrubs has been observed in previous experimental studies ("fertile island" effect, e.g. Schlesinger et al. (1990, 1996); Whitford (2002)), but for other reasons – the complex processes involved are not explicitly implemented in JSBACH.

Another important aspect to be considered is that various factors can affect veg_{max} in coupled simulations apart from precipitation, which is the main determinant of plant growth in semi-arid regions on the considered scale of the order of a GCM grid cell (Coughenour and Ellis, 1993). Two important additional factors appear upon closer inspection of the outliers in Fig. 4. First, shallow soils in mountainous regions (in JSBACH, compare Fig. 1) are not capable of holding water and therewith impede plant growth despite high precipitation. Second, in regions where temperatures of the coldest month fall below the bioclimatic threshold of TE/TD (15.5°C), these tropical PFTs cannot establish thereby favoring the dominance of other PFTs with different water requirements. This effect is substantially reduced in EXP_{TD10} with the implementation of a frost tolerant Tropical Tree PFT.

3.2 Effects on the transition from the "green" Sahara to the "desert" state

For a first estimate of regional transition patterns from the "green" Sahara (8 ky) to the "desert" state (0 ky), we ~~subtract 100-year averages of~~ calculate differences between consecutive time slices (8 ky-6 ky, 6 ky-4 ky, 4 ky-2 ky, 2 ky-0 ky) of the 100-year averages of P and veg_{max} for all simulations, and compare the resulting transition maps of P and veg_{max} in the whole study domain (~~12~~11.19 to ~~34~~33.57° N, ~~-15 to 40~~15.94° W to 40.31° E). Note that this analysis does not represent the transient changes of vegetation extent and precipitation over the last 8000 years but provides an estimate of possible different states for a series of external forcings. This set up implies vegetation being permanently in equilibrium with climate. In reality, the delayed response of vegetation allows several potential transient conditions to exist before diversity slowly attains equilibrium (Vellend et al., 2006; Diamond, 1972; Brooks et al., 1999). However, as the time scales of the simulated vegetation dynamics and atmospheric processes are much shorter than the 2 ky period between simulated time slices, this approach is legitimate for this study.

In EXP_{ALL}, the western part of the study domain experiences a stronger precipitation reduction than the eastern part in all periods (Fig. 5, left column). The latitudes of strongest precipitation decline shift gradually southward indicating a southward shift of the tropical rain belt over time. A slight precipitation increase at the southwestern coast in the first period before precipitation starts decreasing in concert with the rest of the domain supports this indication. The magnitude of P decline ranges from less than 50 mm yr^{-1}(2 ky)$^{-1}$ in the northern part of the domain to more than 200 mm yr^{-1}(2 ky)$^{-1}$ at the latitudes of maximum change between around 12 and 20° N, with single grid cells in the western part reaching up to 250 mm yr^{-1}(2 ky)$^{-1}$. veg_{max} follows the pattern of P decline with a latitudinal offset of around one grid cell to the north, reaching maximum rates of decrease from 0.1 to 0.2 yr^{-1}(2 ky)$^{-1}$ in the transition zone between desert and savanna (Fig. 5, right column). This transition zone shifts southward from about 18 to 22° N at 8 ky to around 14 to 20° N at 0 ky. The latitudinal offset indicates that vegetation does not respond directly to changes in P but declines when a threshold is reached at low precipitation rates. The almost constant rates of P and veg_{max} decline in the latitudes of maximum change in all periods represent a gradual transition from the “green” Sahara to the “desert” state.

The simulations with modified PFT diversity show qualitatively similar patterns of P and veg_{max} decline (see appendix). However, the timing and rate of transition substantially differ between simulations with different PFT compositions.

For the quantitative comparison of all simulations, we condense the information of the transition maps by calculating zonal means (~~-15 to 40~~15.94 ° W to 40.31° E) of P and veg_{max} ~~,~~and subtracting consecutive time slices. These zonally averaged differences between consecutive time slices are in the following referred to as ΔP and Δveg_{max}. Figure 6 illustrates that the maximum as well as the temporal evolution of ΔP and Δveg_{max} considerably differ between simulations.

Just as described above for the transition maps, the latitudes of maximum change shift in EXP_{ALL} gradually southward by one grid cell per period (Fig. 6a). Δveg_{max} follows the symmetric pattern of ΔP with a meridional offset of around one grid cell to the north, reaching maximum rates of decrease in the transition zone between desert and savanna (Fig. 6b). In EXP_{C4}, $EXP_{TE,C4}$, and EXP_{TD10}, the temporal evolutions of ΔP and Δveg_{max} exhibit a delayed and sharpened transition compared to EXP_{ALL} (Fig. 6c-f, i-j), whereas $EXP_{SRG,C4}$ depicts a delayed but smoothed transition (Fig. 6g, h). Δveg_{max} shows in $EXP_{SRG,C4}$ an exceptional behavior with a slow but non-monotonous southward shift of the most changing latitudes.

The explanation for differences in timing and magnitude of vegetation and precipitation decline between simulations with different PFT compositions is twofold. The first part of the explanation lies in dissimilar initial precipitation and vegetation cover fraction values. High initial values of P and veg_{max} in EXP_{C4}, $EXP_{TE,C4}$, and EXP_{TD10} in the transition zone between desert and savanna imply a large gradient between “green” and “desert” state and therewith inherit a larger potential for high ΔP and Δveg_{max} than EXP_{ALL} and $EXP_{SRG,C4}$ (Fig. 2, Tab. 3). In other words, if the initial values are low, there is no potential to show a decrease as large as starting from a higher value.

The second part of the explanation lies in the disparate relationships between precipitation and vegetation cover fraction and in the associated different sensitivities to precipitation decline that are specific to the particular PFT composition, depicted in the vegetation–precipitation diagrams (V–P diagrams) in Fig. 4 for all simulations at 8 ky (blue) and 0 ky (red) including all grid cells in the study domain to cover the full precipitation spectrum.

If we consider a grid cell j at the upper end of the ~~dominant branch~~ precipitation range in any simulation, the qualitatively constant relationship between P and veg_{max} over time indicates that $veg_{max,j}$ “moves” left along the branch in the V–P diagram when P_j declines. Within a certain precipitation range, $veg_{max,j}$ is not affected by a precipitation reduction until the threshold of maximum cover is reached. The position of this threshold is determined by the ratio of involved PFTs resulting from competition, their productivities and capabilities to suppress desert expansion as described earlier in Sect.3.2. When P_j drops below the threshold of maximum cover, $veg_{max,j}$ starts to decrease according to the slope of the branch. If the threshold value is low, the slope of the branch is steep, and $veg_{max,j}$ drops abruptly with a small precipitation decline. If the threshold value is higher, the slope is shallower, and $veg_{max,j}$ retreats more gradually. ~~The~~ Thus, the regional response is ~~determined by the dominant branch, therewith~~ sharp in EXP_{C4}, $EXP_{TE,C4}$, and EXP_{TD10}, gradual in EXP_{ALL}, and very shallow in $EXP_{SRG,C4}$. With further precipitation decline below the threshold, not only $veg_{max,j}$ decreases, but the PFT composition changes as well. PFTs with high moisture requirements cannot sustain growth and are consequently replaced by more drought resistant PFTs. The alteration in PFT composition implies that the relationship between P_j and $veg_{max,j}$ changes in the respective grid cell, thus the grid cell value "jumps" to another branch and follows its trajectory with further precipitation decrease. This jump happens most obviously in $EXP_{SRG,C4}$. When SRG disappears after 4 ky and thereby allows $C4$ to establish, affected grid cells shift to the upper branch in the diagram, which resembles the main branch of EXP_{C4}, and reach a higher cover fractions with the same precipitation amount. This shift also explains the non-monotonous vegetation retreat in Fig. 6h.

4 Discussion

The present study is a first attempt to account for effects of plant functional diversity on climate–vegetation interaction in a comprehensive Earth system model. Our results confirm previous conceptual studies on the effect of plant diversity on climate–vegetation interaction (Claussen et al., 2013; Groner et al., 2015) in accordance with the "diversity-stability" hypothesis (McCann, 2000; Scherer-Lorenzen, 2005): high diversity can smooth the vegetation response to an externally forced precipitation decline, as we demonstrate in the comparison between EXP_{ALL} and EXP_{C4}/$EXP_{TE,C4}$. Our findings thereby reconcile a gradual transition from a "green" state to a "desert" state with a strong feedback between ~~single plant types~~ vegetation and climate. On the other hand, the removal or introduction of key stone species – here SRG or TD_{10} respectively – can substantially alter the vegetation response to an externally forced precipitation decline. Despite the potential PFT diversity is highest in EXP_{TD10}, the properties of realized PFTs change the vegetation dynamics and the interaction with the atmosphere such that the transition happens with a similar fast rate as in the simulation with only one PFT (EXP_{C4}). In contrast, the dominance of the desert promoting SRG in $EXP_{SRG,C4}$ leads to a transition that is even more gradual than in the experiments with higher potential PFT diversity. Thus, not the absolute number of potential PFTs, but the realized PFT composition determines climate–vegetation interaction and the system response to changing external forcing.

Previous studies have shown that the differences in the strength of climate vegetation coupling contribute to the differences in the extent of the "green" Sahara in different models. The sensitivity of the simulated system to changes in PFT composition and PFT properties could be an additional explanation why previous studies showed different extents of the "green" Sahara (see Claussen et al., 2017). Some land surface models such as ORCHIDEE (Krinner et al., 2005) do not have a Raingreen Shrub PFT which plays a crucial role in competition in JSBACH, especially in the transition zone between desert and savanna. Further, the definition of bioclimatic limits in terms of minimum temperature of the coldest month, which is set to 15.5°C in many land surface models, prevents tropical tree PFTs from establishment in regions where they were reconstructed for the AHP. With the significant increase of vegetation cover fraction north of 20° N, the simulation with a frost tolerant tropical tree EXP_{TD10} reaches a closer match to reconstructions than previous studies. The final choice of this bioclimatic limit requires further investigation.

Eventually, our findings raise the question how plant functional diversity should generally be represented in land surface models to obtain a functionally realistic description of vegetation. The PFT concept is the most commonly used approach to represent vegetation in the current generation of DGVMs, but its validity has been extensively discussed over the last years. The representation of plant diversity with a static set of discrete PFT parameters does not cover the range of species categorized as one PFT and disregards phenotypic plasticity and trait variability (Van Bodegom et al., 2012; Wullschleger et al., 2014) which are often larger within PFTs than between PFTs (de Bello et al., 2011; Kattge et al., 2011).

Alternative approaches to represent plant diversity consider the simulation of individual plants (e.g. LPJ-GUESS (Smith et al., 2001); aDGVM (Scheiter et al., 2013)), ~~trail variability~~“trait variability” which allows selected traits to vary within the range of observations to optimize growth under varying environmental conditions (e.g. JSBACH (Verheijen et al., 2013, 2015)), ~~trait flexibility~~ “trait flexibility” which represents plant diversity in terms of plant ecophysiological trade-offs instead of PFTs by selecting for the most suitable growth strategy out of randomly generated sets of parameter values (e.g. JeDi-DGVM (Pavlick, 2012); aDGVM (Scheiter et al., 2013)), or operate based on the “evolutionary optimality hypothesis~~(Wang et al., 2017).~~”, an approach based on the microeconomic standard framework to determine the optimal input mix for a two-input production process, here water loss and carbon gain during photosynthesis (Wang et al., 2017).

Nevertheless, the PFT concept remains the current standard method to represent vegetation in land surface models, and we suggest that the uncertainties arising from the incomplete representation of plant diversity need to be taken into account in the interpretation of modelling studies.

5 Summary and Conclusions

In the present study, we have illustrated how variations in plant functional diversity affect climate–vegetation interaction towards the end of the AHP in coupled land-atmosphere simulations.

In experiments with AHP boundary conditions, the extent of the “green” Sahara varies considerably with changes in plant functional diversity. Differences in vegetation extent and PFT composition in turn alter land surface parameters, water cycling and the surface energy budget. These changes have not only local consequences but significantly affect large scale atmospheric circulation patterns indicating a strong feedback between the terrestrial biosphere and the atmosphere. In contrast with the general hypothesis of a positive climate–vegetation feedback, we find that higher vegetation cover is not necessarily associated with higher precipitation but determined by the properties of the predominant PFTs which are highly model dependent. We demonstrate that the simulated climate–vegetation system state is highly sensitive to the implementation of these properties by the example of bioclimatic limits in terms of minimum temperature of the coldest month for the PFT “Tropical Deciduous Tree”.

Towards the end of the AHP, modifications of PFT diversity significantly impact the timing and rate of transition to the "desert" state. While the simulations with the standard PFT set in MPI-ESM show a gradual decrease of precipitation and vegetation cover over time, variations in potential PFT diversity cause either a sharp decline of both variables or an even slower response to the external forcing depending on the realized PFT composition. The explanation lies in different initial precipitation and vegetation cover values as well as in different relationships between precipitation and vegetation cover fraction that are specific to the particular PFT composition.

Recapitulatory, we identify the realized PFT diversity rather than the potential PFT diversity as the decisive factor for climate–vegetation feedback strength, vegetation extent, and the timing and rate of transition from the "green" Sahara to the "desert" state in MPI-ESM. Since climate–vegetation interaction is highly sensitive to the PFT composition and the model-specific PFT representation, we expect that the observed effects are not limited to the subtropics during the mid-Holocene, but could occur in different regions, especially in transition zones between different biomes, under different external forcings, including recent and future climate change. This raises the question how realistically Earth system models can actually represent climate–vegetation interaction, considering the poor representation of plant diversity in the current generation of land surface models. However, as long as the processes shaping ecosystems are still not fully understood, it remains a challenge to set the criteria for an appropriate representation of plant functional diversity in land surface models.

Acknowledgements. We thank Victor Brovkin for internal review and fruitful discussions, and the anonymous referees for insightful comments.
The article processing charges for this open-access publication were covered by the Max Planck Society.

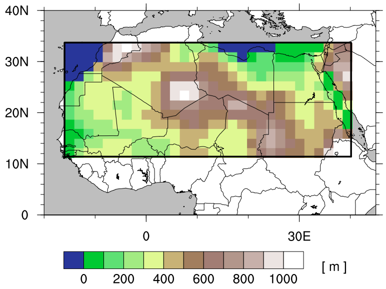

Figure 1. Mean orography (in m) of the simulated study domain in north Africa, ~~12~~11.19 to ~~34~~33.57° N, ~~-15~~ 15.94° W to ~~40~~40.31° E.

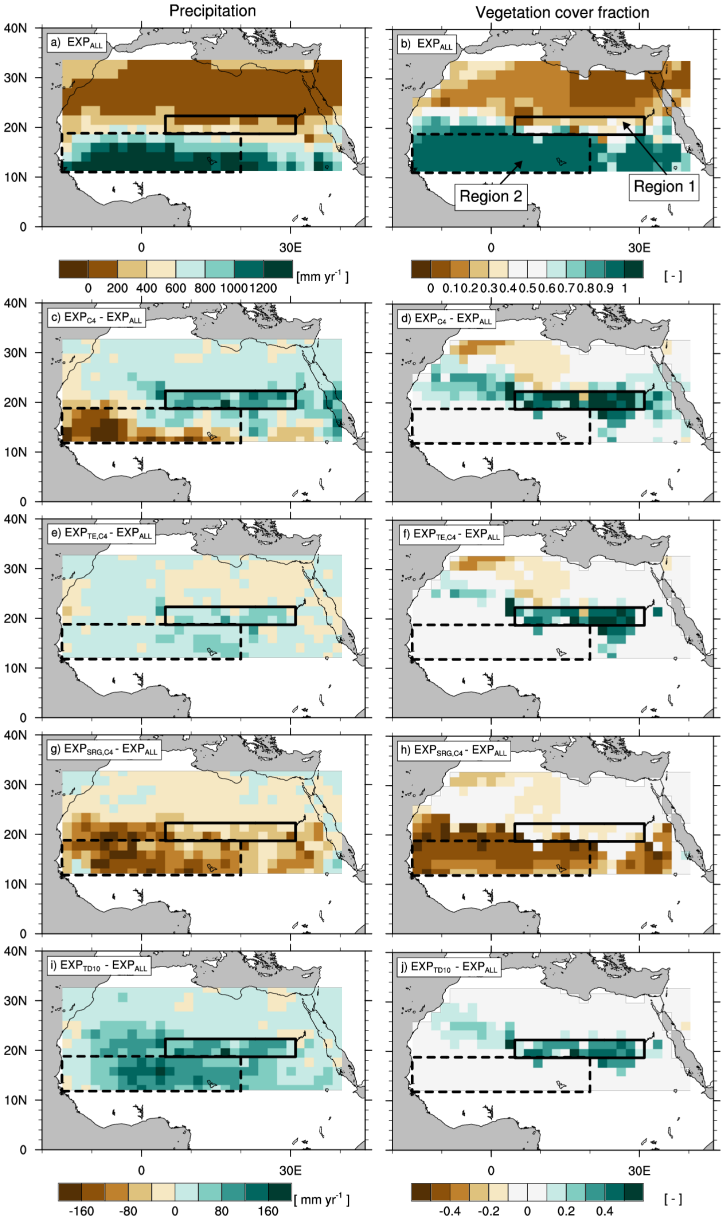

Figure 2. Effects of changes in plant functional diversity on precipitation P (left column) and vegetation cover fraction veg_{max} (right column) during the AHP (8 ky) in Region 1 (~~18~~18.65 to ~~22~~22.38° N, ~~5~~4.69 to ~~30~~30.94° E, solid box) and Region 2 (~~12~~11.19 to ~~18~~18.65° N, ~~-15~~15.94$circ$ W to ~~20~~19.69° E, dashed box). Panels (a, b) show 100-year averages for the experiment with the standard PFT set (EXP_{ALL}). The following panels illustrate differences in 100-year averages between EXP_{ALL} and EXP_{C4} (c, d), $EXP_{TE,C4}$ (e, f), $EXP_{SRG,C4}$ (g, h), and EXP_{TD10} (i, j).

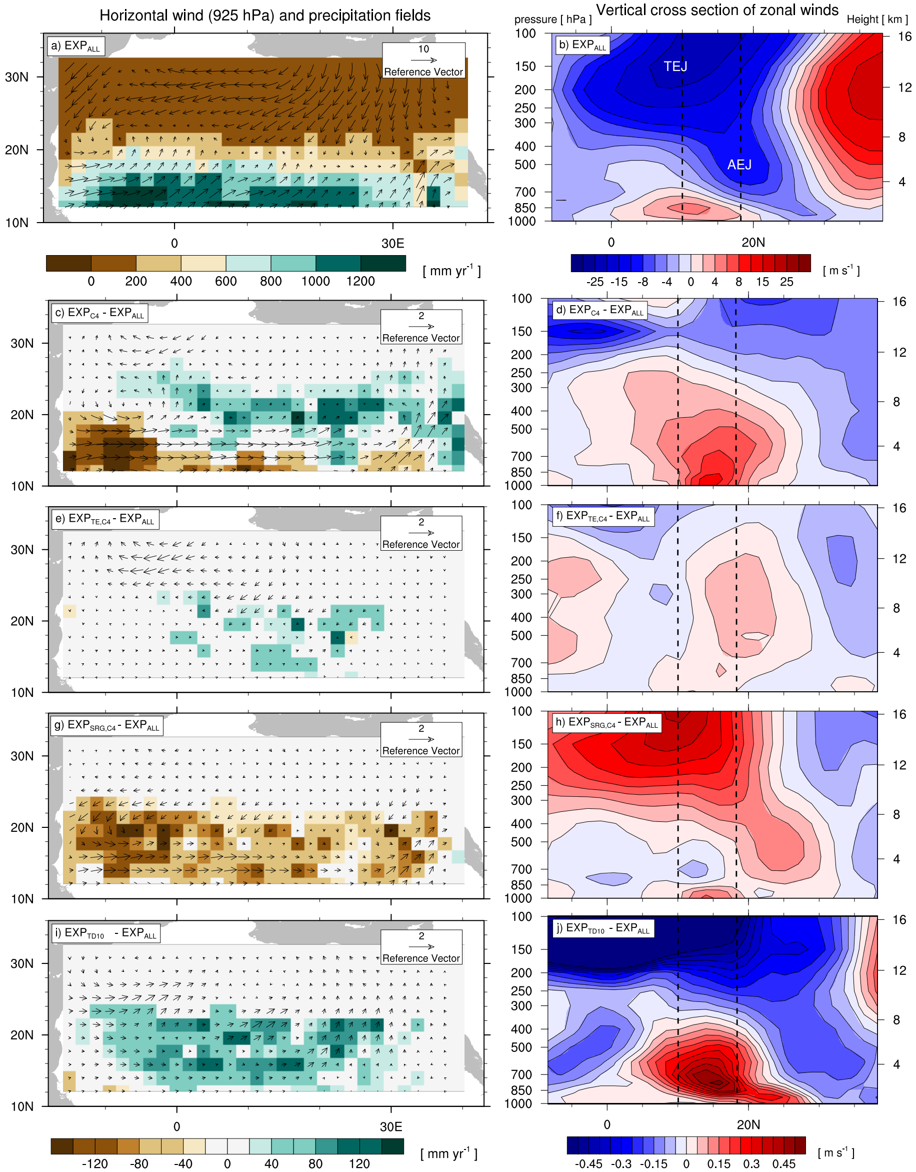

Figure 3. Effects of changes in plant functional diversity on precipitation P and large scale atmospheric circulation patterns during the monsoon season (JJAS) under AHP conditions (8 ky). Left: horizontal low-level wind fields in the monsoon layer (925 hPa) and P fields. Right: vertical cross sections of zonal winds (~~-10~~9.33 to ~~40~~39.17° N, ~~-10~~10.31° W to ~~40~~40.31° E). Dotted lines mark the core regions of mid-level African Easterly Jet (AEJ, 600 hPa) and upper-level Tropical Easterly Jet (TEJ, 150 hPa) in EXP_{ALL}. Panels (a, b) show the 100-year average for the experiment with the standard PFT set (EXP_{ALL}), the following panels illustrate differences in 100-year averages between EXP_{ALL} and EXP_{C4} (c, d), $EXP_{TE,C4}$ (e, f), $EXP_{SRG,C4}$ (g, h), and EXP_{TD10} (i, j).

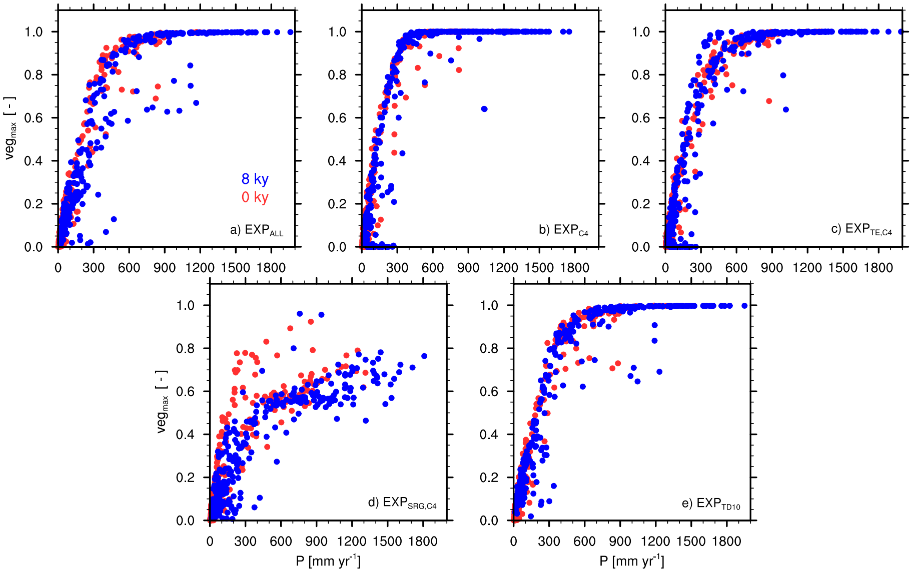

Figure 4. Vegetation–precipitation diagrams (veg_{max}, P) for simulations with different PFT combinations including all grid cells in the study domain (~~12~~11.19 to ~~34~~33.57° N, ~~-15~~ -15.94° W to ~~40~~40.31° E). Values are derived from 100-year averages under 8 ky (blue) and 0 ky (red) boundary conditions for EXP_{ALL} (a), EXP_{C4} (b), $EXP_{TE,C4}$ (c), $EXP_{SRG,C4}$ (d), and EXP_{TD10} (f) .

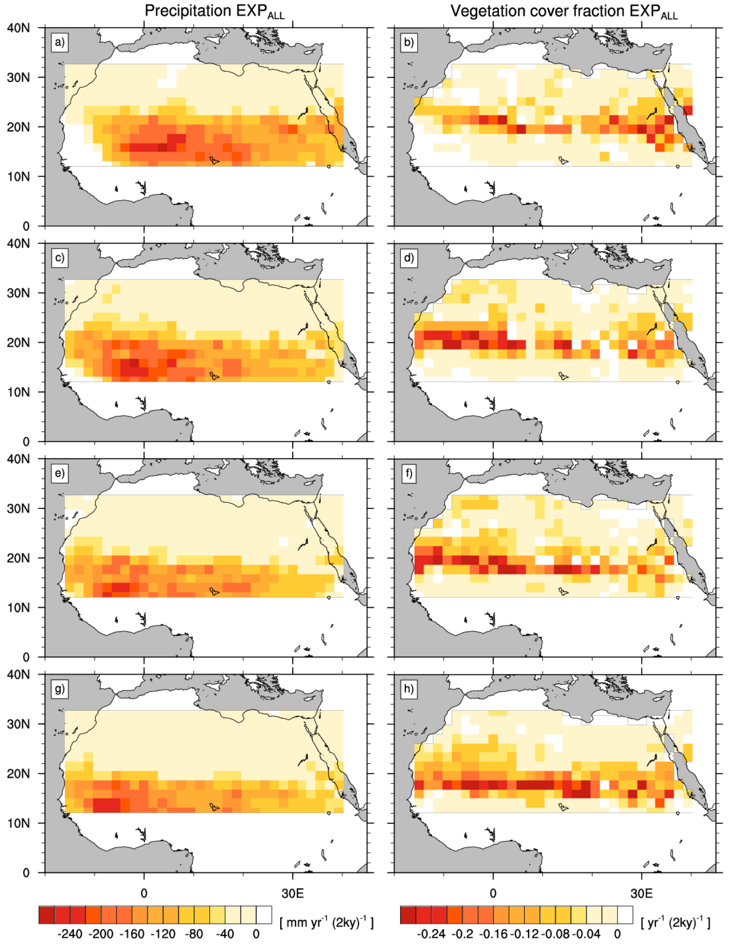

Figure 5. Transition rates from the “green” Sahara to the “desert” state for precipitation P (left column) and vegetation cover fraction veg_{max} (right column) of a simulation with the standard PFT set (EXP_{ALL}). Plots depict differences between consecutive time slices (100-year averages): 6 ky-8 ky (a, b), 4 ky-6 ky (c, d), 2 ky-4 ky (e, f), and 0 ky-2 ky (g, h).

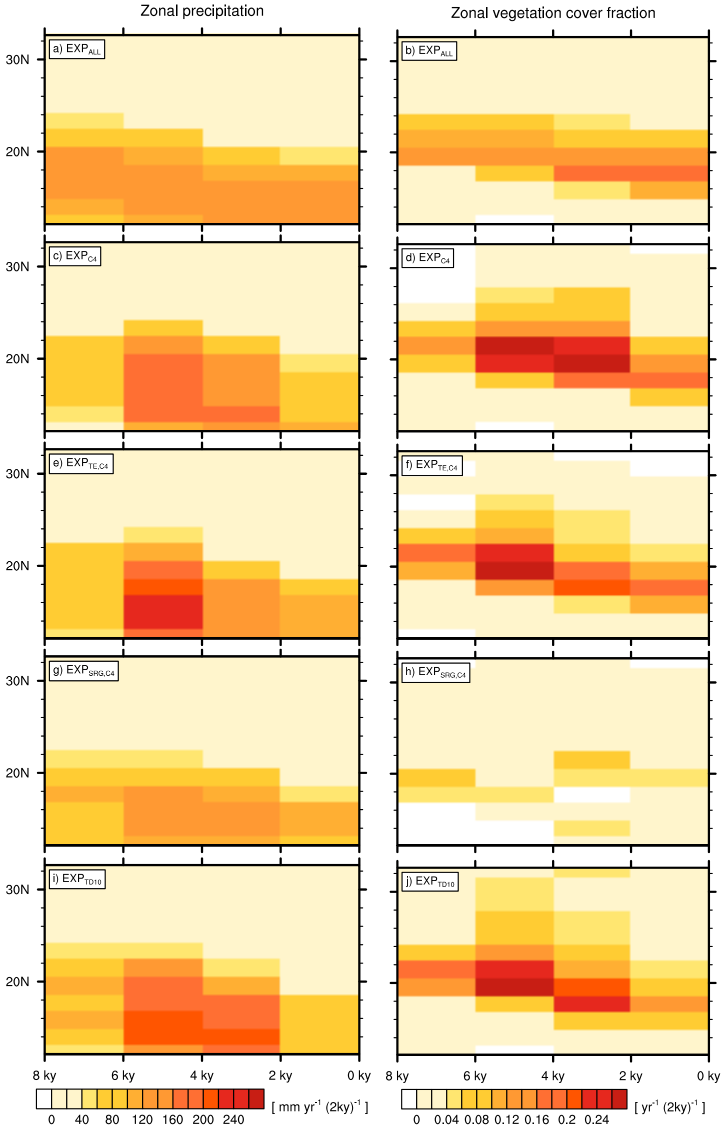

Figure 6. Zonally averaged transition rates from the "green" Sahara to the "desert" state for precipitation ΔP_i (left column) and vegetation cover fraction $\Delta veg_{max,i}$ (right column). Plots depict differences between consecutive time slices (100-year averages) for EXP_{ALL} (a, b), EXP_{C4} (c, d), $EXP_{TE,C4}$ (e, f), $EXP_{SRG,C4}$ (g, h), and EXP_{TD10} (i, j).

Table 1. Natural Plant Functional Types in JSBACH, their woodiness type, associated time constants for establishment/mortality (τ_i, in years), maximum carboxylation capacities ($V_{max,0,i}$) and electron transport capacities ($J_{max,0,i}$) at 25 °C (in μmol(CO$_2$) m^{-2} s^{-1}), specific leaf area (SLA_i, in m^2(leaf) mol^{-1}(Carbon)), ~~and~~ maximum leaf area index ($LAI_{max,i}$, in m^2 m^{-2}), canopy albedo α in VIS/NIR, and vegetation roughness length z_0 (in m] (Reick et al., 2013).

Plant Functional Type	ID	type	τ_i	$V_{max,0,i}$	$J_{max,0,i}$	SLA_i	$LAI_{max,i}$	$\alpha_{VIS,i}$	$\alpha_{NIR,i}$	$z_{0,i}$
Tropical Evergreen Tree	TE	woody	30	39	74.1	0.264	7	0.3	0.22	2.0
Tropical Deciduous Tree	TD	woody	30	31	59.8	0.376	7	0.4	0.23	1.0
Extra-trop. Evergreen Tree	eTE	woody	60	44	83.6	0.110	5	0.4	0.23	1.0
Extra-trop. Deciduous Tree	eTD	woody	60	66	125.4	0.304	5	0.5	0.26	1.0
Raingreen Shrub	SRG	woody	12	61.7	117.2	0.184	2	0.05	0.25	0.5
Deciduous Shrub	SD	woody	24	54	102.6	0.307	2	0.05	0.28	0.5
C3 Grass	$C3$	grass	1	78.2	148.6	0.451	3	0.08	0.33	0.05
C4 Grass	$C4$	grass	1	8	140	0.451	3	0.08	0.33	0.05

Table 2. CO$_2$ concentrations (in ppm) and orbital parameters for simulated time slices at 8 ky, 6 ky, 4 ky, 2 ky, and 0 ky. For palaeo simulations, CO$_2$ concentrations are taken from Joos (2016) and orbital parameters are adjusted according to Berger (1978). The values for 0 ky conform to the standard preindustrial set up of MPI-ESM.

time slice	CO$_2$ [ppm]	eccentricity [-]	obliquity [-]	longitude of perihelion [°]
8 ky	259.9	0.019101	24.209	148.58
6 ky	264.6	0.01867	24.101	181.75
4 ky	273.2	0.018123	23.922	215.18
2 ky	277.6	0.017466	23.694	248.93
0 ky	284.725	0.016704	23.44	283.01

Table 3. Effects of different PFT compositions on land surface parameters, surface energy budget, and hydrological cycle in coupled land-atmosphere simulations in Region 1 (~~18~~18.65 to ~~22~~22.38° N, ~~5~~4.69 to ~~30~~30.94° E) and Region 2 (~~12~~11.19 to ~~18~~18.65° N, ~~-15~~15.94° W to ~~20~~19.69° E). The first two columns contains 100-year averages of the experiment with the standard PFT set EXP_{ALL}, the following show differences between EXP_{ALL} and simulations with modified PFT composition (Tropical Evergreen Tree TE, Raingreen Shrub SRG, C4 Grass $C4$, frost tolerant Tropical Deciduous Tree TD_{10}). Bold values are significant (σ = 0.05) with regard to the time series of 100 years (yearly averages), values in brackets correspond to spatial standard deviations of difference fields.

	EXP_{ALL}		EXP_{C4} - EXP_{ALL}		$EXP_{TE,C4}$ - EXP_{ALL}		$EXP_{SRG,C4}$ - EXP_{ALL}		EXP_{TD10} - EXP_{ALL}	
	Region 1	Region 2	Region 1	Region 2	Region 1	Region 2	Region 1	Region 2	Region 1	Region 2
Land surface parameters										
Vegetation cover fraction [-]	0.40(0.22)	0.98(0.04)	**0.44**(0.21)	**0.02**(0.04)	**0.34**(0.21)	**0.01**(0.04)	**-0.12**(0.13)	**-0.40**(0.08)	**0.31**(0.16)	**0.01**(0.04)
Leaf area index [m^2(leaf) m^{-2}(canopy)]	1.33(0.43)	3.00(0.7)	**0.18**(0.33)	**-0.43**(0.38)	0.03(0.32)	0.02(0.04)	**-0.30**(0.17)	**-1.11**(0.57)	**0.15**(0.15)	**0.09**(0.06)
Albedo [-]	0.28(0.07)	0.17(0.01)	**-0.07**(0.06)	**0.02**(0.01)	**-0.06**(0.05)	**-0.001**(0.001)	**0.03**(0.04)	**0.01**(0.02)	**-0.07**(0.06)	**-0.001**(0.001)
Roughness length [m]	0.08(0.07)	1.32(0.69)	**-0.03**(0.07)	**-1.24**(0.68)	**0.03**(0.09)	**0.07**(0.09)	**-0.04**(0.06)	**-1.19**(0.64)	**0.13**(0.07)	**0.11**(0.10)
Surface energy budget										
Solar net radiation [W m^{-2}]	275.26(14.03)	289.79(3.95)	**12.33**(12.00)	**-2.62**(1.46)	**10.78**(10.37)	0.005(0.34)	**-4.76**(7.24)	**1.11**(4.24)	**11.55**(11.10)	**-0.85**(0.55)
Sensible heat flux [W m^{-2}]	61.88(10.55)	47.18(17.15)	**6.38**(11.00)	**-1.36**(3.82)	**7.17**(9.10)	-0.32(0.68)	**-3.77**(6.26)	**2.54**(5.23)	**9.90**(10.42)	**-2.09**(1.1)
Latent heat flux [W m^{-2}]	20.07(7.88)	70.12(22.70)	**5.21**(2.88)	**-6.27**(4.75)	**2.17**(2.29)	0.53(0.88)	**-4.31**(2.74)	**-7.63**(3.72)	**5.64**(2.26)	**2.41**(1.31)
2 m temperature [°C]	24.95(1.54)	26.21(1.42)	**0.46**(0.28)	**0.47**(0.21)	**0.50**(0.29)	0.04(0.07)	-0.07(0.11)	**0.73**(0.28)	**0.37**(0.29)	-0.07(0.08)
Cloud cover [-]	0.35(0.04)	0.53(0.06)	0.01(0.002)	**-0.02**(0.01)	0.003(0.002)	-0.002(0.004)	**-0.02**(0.003)	**-0.03**(0.003)	**0.02**(0.005)	0.01(0.004)
Hydrological cycle										
Precipitation [mm yr^{-1}]	275.58(104.64)	1140.86(352.69)	**84.87**(34.72)	**-76.19**(83.79)	**35.24**(28.97)	24.81(17.03)	**-56.11**(33.16)	**-110.25**(45.96)	**82.73**(33.88)	**82.88**(40.40)
Evapotranspiration [mm yr^{-1}]	253.31(99.45)	884.82(286.44)	**65.76**(36.30)	**-79.16**(59.91)	**27.50**(28.84)	6.69(11.10)	**-54.33**(34.55)	**-96.23**(46.88)	**71.29**(28.56)	**30.37**(16.58)
Integrated water vapor [kg m^2]	20.49(1.86)	32.62(3.52)	**0.62**(0.09)	**-0.40**(0.47)	0.09(0.08)	0.09(0.09)	**-0.95**(0.24)	**-1.40**(0.16)	**0.84**(0.30)	**0.73**(0.23)

Table 4. Mean cover fractions f_i (per vegetated area of a grid cell) of all Plant Functional Types (PFTs) with substantial shares of the total vegetation cover in Region 1 (~~18~~18.65 to ~~22~~22.38° N, ~~5~~4.69 to ~~30~~30.94° E) and Region 2 (~~12~~11.19 to ~~18~~18.65° N, ~~-15~~15.94° W to ~~20~~19.69° E). Values represent 100-year averages of the experiment with the standard PFT set EXP_{ALL} and simulations with modified PFT composition (Tropical Evergreen Tree TE, Raingreen Shrub SRG, C4 Grass $C4$, frost tolerant Tropical Deciduous Tree TD_{10}).

	EXP_{ALL}		EXP_{C4}		$EXP_{TE,C4}$		$EXP_{SRG,C4}$		EXP_{TD10}	
PFT	Region 1	Region 2	Region 1	Region 2	Region 1	Region 2	Region 1	Region 2	Region 1	Region 2
TE	0.01	0.40	-	-	0.05	0.42	-	-	0.01	0.42
TD	0.02	0.01	-	-	-	-	-	-	<0.01	<0.01
$TD10$	-	-	-	-	-	-	-	-	0.20	<0.01
SRG	0.14	0.01	-	-	-	-	0.18	0.34	0.01	<0.01
$C4$	0.20	0.57	0.84	1.0	0.69	0.57	0.1	0.25	0.48	0.55

Appendix A

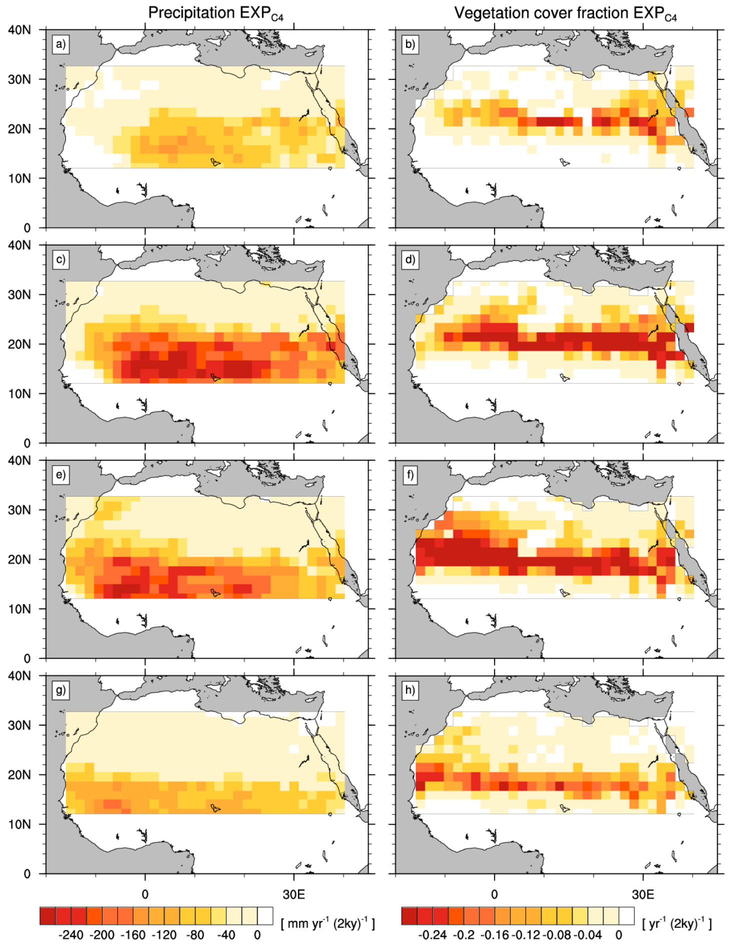

Figure A1. Transition rates from the “green” Sahara to the “desert” state for precipitation P (left column) and vegetation cover fraction veg_{max} (right column) of a simulation with C4 Grass only (EXP_{C4}). Plots depict differences between consecutive time slices (100-year averages): 6 ky-8 ky (a, b), 4 ky-6 ky (c, d), 2 ky-4 ky (e, f), and 0 ky-2 ky (g, h).

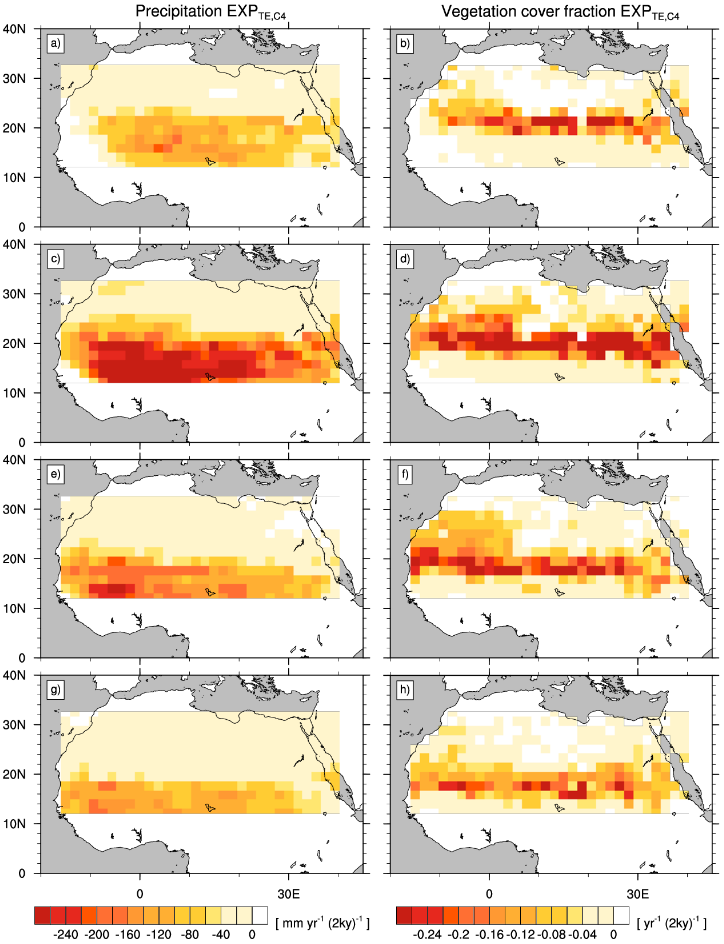

Figure A2. Transition rates from the "green" Sahara to the "desert" state for precipitation P (left column) and vegetation cover fraction veg_{max} (right column) of a simulation with C4 Grass and Tropical Evergreen Tree ($EXP_{TE,C4}$). Plots depict differences between consecutive time slices (100-year averages): 6 ky-8 ky (a, b), 4 ky-6 ky (c, d), 2 ky-4 ky (e, f), and 0 ky-2 ky (g, h).

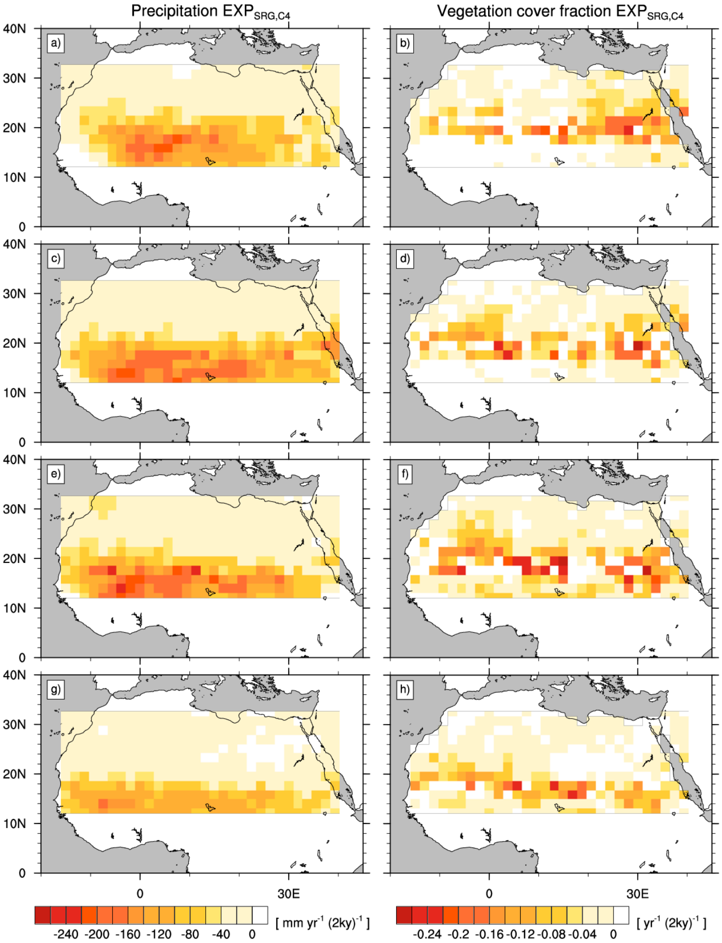

Figure A3. Transition rates from the "green" Sahara to the "desert" state for precipitation P (left column) and vegetation cover fraction veg_{max} (right column) of a simulation with C4 Grass and Raingreen Shrub ($EXP_{SRG,C4}$). Plots depict differences between consecutive time slices (100-year averages): 6 ky-8 ky (a, b), 4 ky-6 ky (c, d), 2 ky-4 ky (e, f), and 0 ky-2 ky (g, h).

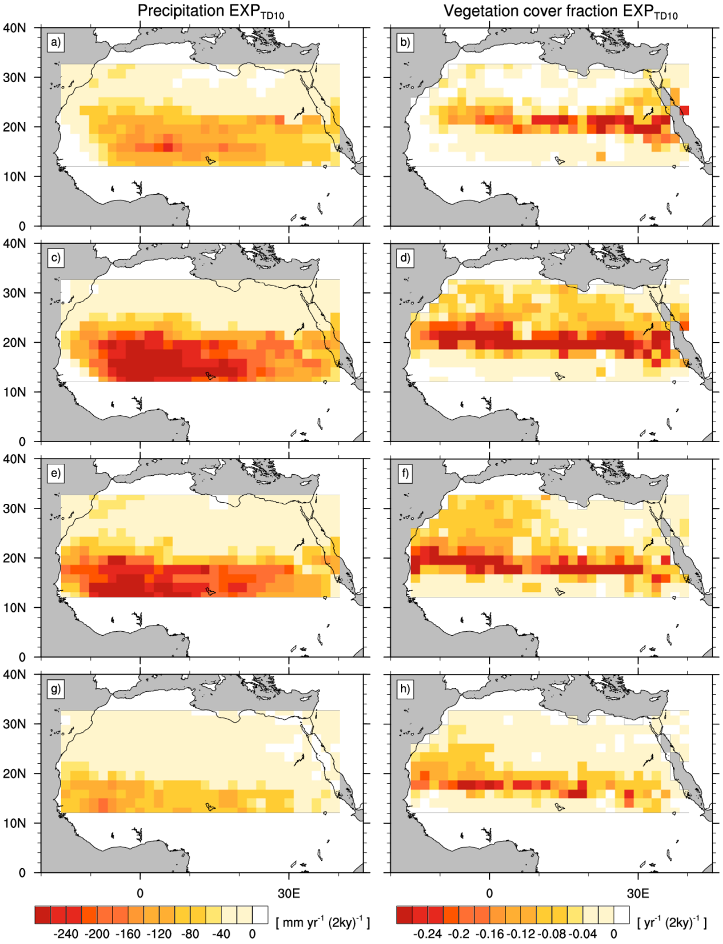

Figure A4. Transition rates from the “green” Sahara to the “desert” state for precipitation P (left column) and vegetation cover fraction veg_{max} (right column) of a simulation with the standard PFT set and a newly designed frost tolerant Tropical Deciduous Tree PFT (EXP_{TD10}). Plots depict differences between consecutive time slices (100-year averages): 6 ky-8 ky (a, b), 4 ky-6 ky (c, d), 2 ky-4 ky (e, f), and 0 ky-2 ky (g, h).

References

Bartlein, P. J., Harrison, S. P., Brewer, S., Connor, S., Davis, B. A. S., Gajewski, K., Guiot, J., Harrison-Prentice, T. I., Henderson, A., Peyron, O., Prentice, I. C., Scholze, M., Seppä, H., Shuman, B., Sugita, S., Thompson, R. S., Viau, A. E., Williams, J., and Wu, H.: Pollen-based continental climate reconstructions at 6 and 21 ka: a global synthesis, Clim. Dyn., 37, 775–802, doi:10.1007/s00382-010-0904-1, https://doi.org/10.1007/s00382-010-0904-1, 2011.

Bathiany, S., Claussen, M., Brovkin, V., Raddatz, T., and Gayler, V.: Combined biogeophysical and biogeochemical effects of large-scale forest cover changes in the MPI earth system model, Biogeosciences, 7, 1383–1399, doi:10.5194/bg-7-1383-2010, https://www.biogeosciences.net/7/1383/2010/, 2010.

Bathiany, S., Claussen, M., and Fraedrich, K.: Implications of climate variability for the detection of multiple equilibria and for rapid transitions in the atmosphere-vegetation system, Clim. Dyn., 38, 1775–1790, doi:10.1007/s00382-011-1037-x, https://doi.org/10.1007/s00382-011-1037-x, 2012.

Berger, A. L.: Long-term variations of caloric insolation resulting from the earth's orbital elements, Quat. Res., 9, 139–167, doi:10.1016/0033-5894(78)90064-9, http://www.sciencedirect.com/science/article/pii/0033589478900649, 1978.

Bonfils, C., de Noblet-Ducoudré, N., Braconnot, P., and Joussaume, S.: Hot Desert Albedo and Climate Change: Mid-Holocene Monsoon in North Africa, J. Clim., 14, 3724–3737, doi:10.1175/1520-0442(2001)014<3724:HDAACC>2.0.CO;2, http://dx.doi.org/10.1175/1520-0442(2001)014<3724:HDAACC>2.0.CO;2, 2001.

Braconnot, P., Joussaume, S., Marti, O., and de Noblet, N.: Synergistic feedbacks from ocean and vegetation on the African Monsoon response to Mid-Holocene insolation, Geophys. Res. Lett., 26, 2481–2484, doi:10.1029/1999GL006047, 1999.

Brooks, T. M., Pimm, S. L., and Oyugi, J. O.: Time lag between deforestation and bird extinction in tropical forest fragments, Conserv. Biol., 13, 1140–1150, doi:10.1046/j.1523-1739.1999.98341.x, 1999.

Brovkin, V., Claussen, M., Petoukhov, V., and Ganopolski, A.: On the stability of the atmosphere–vegetation system in the Sahara/Sahel region, J. Geophys. Res.-Atmos., 103, 31 613–31 624, doi:10.1029/1998JD200006, 1998.

Brovkin, V., Raddatz, T., Reick, C. H., Claussen, M., and Gayler, V.: Global biogeophysical interactions between forest and climate, Geophys. Res. Lett., 36, Seq. No.: L07 405, 2009.

Claussen, M.: On coupling global biome models with climate models, Clim. Res., 4, 203–221, 1994.

Claussen, M. and Gayler, V.: The greening of the Sahara during the Mid-Holocene: results of an interactive atmosphere–biome model, Global Ecol. Biogeogr., 6, 369–377, doi:10.2307/2997337, 1997.

Claussen, M., Kubatzki, C., Brovkin, V., Ganopolski, A., Hoelzmann, P., and Pachur, H.-J.: Simulation of an abrupt change in Saharan vegetation in the Mid-Holocene, Geophys. Res. Lett., 26, 2037–2040, doi:10.1029/1999GL900494, 1999.

Claussen, M., Bathiany, S., Brovkin, V., and Kleinen, T.: Simulated climate–vegetation interaction in semi-arid regions affected by plant diversity, Nat. Geosci., 6, 954–958, doi:10.1038/ngeo1962, 2013.

Claussen, M., Dallmeyer, A., and Bader, J.: Theory and Modeling of the African Humid Period and the Green Sahara, doi:10.1093/acrefore/9780190228620.013.532, //climatescience.oxfordre.com/10.1093/acrefore/9780190228620.001.0001/acrefore-9780190228620-e-532, 2017.

Coe, M. and Bonan, G.: Feedbacks between climate and surface water in northern Africa during the middle Holocene, J. Geophys. Res., 102, 11 087–11 101, doi:10.1029/97JD00343, 1997.

Coughenour, M. B. and Ellis, J. E.: Landscape and climatic control of woody vegetation in a dry tropical ecosystem: Turkana District, Kenya, J. Biogeogr., 20, 383–398, doi:10.2307/2845587, 1993.

de Bello, F., Lavorel, S., Albert, C. H., Thuiller, W., Grigulis, K., Dolezal, J., Janecek, S., and Leps, J.: Quantifying the relevance of intraspecific trait variability for functional diversity, Methods Ecol. Evol., 2, 163–174, doi:10.1111/j.2041-210X.2010.00071.x, http://dx.doi.org/10.1111/j.2041-210X.2010.00071.x, 2011.

deMenocal, P., Ortiz, J., Guilderson, T., Adkins, J., Sarnthein, M., Baker, L., and Yarusinsky, M.: Abrupt onset and termination of the African Humid Period: rapid climate responses to gradual insolation forcing, Quaternary Sci. Rev., 19, 347–361, doi:10.1016/S0277-3791(99)00081-5, 2000.

Diamond, J. M.: Biogeographic kinetics: estimation of relaxation times for avifauna of southwest Pacific Islands, Proc. Natl. Acad. Sci. U. S. A., 69, 3199–3203, 1972.

Doherty, R., Kutzbach, J., Foley, J., and Pollard, D.: Fully coupled climate/dynamical vegetation model simulations over Northern Africa during the mid-Holocene, Clim. Dynam., 16, 561–573, doi:10.1007/s003820000065, 2000.

Drake, N. A., Blench, R. M., Armitage, S. J., Bristow, C. S., and White, K. H.: Ancient watercourses and biogeography of the Sahara explain the peopling of the desert, P. Natl. Acad. Sci., 108, 458–462, doi:10.1073/pnas.1012231108, 2011.

Egerer, S., Claussen, M., Reick, C., and Stanelle, T.: The link between marine sediment records and changes in Holocene Saharan landscape: simulating the dust cycle, Clim. Past, 12, 1009–1027, doi:10.5194/cp-12-1009-2016, http://www.clim-past.net/12/1009/2016/, 2016.

FAO/UNESCO: Soil map of the world 1:5,000,000, Vols. 1–10, 1974.

Francus, P., von Suchodoletz, H., Dietze, M., Donner, R. V., Bouchard, F., Roy, A.-J., Fagot, M., Verschuren, D., and Kröpelin, S.: Varved sediments of Lake Yoa (Ounianga Kebir, Chad) reveal progressive drying of the Sahara during the last 6100 years, Sedimentology, 60, 911–934, doi:10.1111/j.1365-3091.2012.01370.x, 2013.

Grist, J. P. and Nicholson, S. E.: A Study of the Dynamic Factors Influencing the Rainfall Variability in the West African Sahel, J. Clim., 14, 1337–1359, doi:10.1175/1520-0442(2001)014<1337:ASOTDF>2.0.CO;2, http://dx.doi.org/10.1175/1520-0442(2001)014<1337:ASOTDF>2.0.CO;2, 2001.

Groner, V. P., Claussen, M., and Reick, C.: Palaeo plant diversity in subtropical Africa – ecological assessment of a conceptual model of climate–vegetation interaction, Clim. Past, 11, 1361–1374, doi:10.5194/cp-11-1361-2015, 2015.

Hagemann, S. and Stacke, T.: Impact of the soil hydrology scheme on simulated soil moisture memory, Climate Dynamics, 44, 1731–1750, doi:10.1007/s00382-014-2221-6, https://doi.org/10.1007/s00382-014-2221-6, 2015.

Harrison, S. P., Prentice, I. C., Barboni, D., Kohfeld, K. E., Ni, J., and Sutra, J.: Ecophysiological and bioclimatic foundations for a global plant functional classification, J. Veg. Sci., 21, 300–317, doi:10.1111/j.1654-1103.2009.01144.x, 2010.

Hély, C., Lézine, A.-M., and APD contributors: Holocene changes in African vegetation: tradeoff between climate and water availability, Clim. Past, 10, 681–686, doi:10.5194/cp-10-681-2014, 2014.

Hoelzmann, P., Jolly, D., Harrison, S. P., Laarif, F., Bonnefille, R., and Pachur, H.-J.: Mid-Holocene land-surface conditions in northern Africa and the Arabian Peninsula: a data set for the analysis of biogeophysical feedbacks in the climate system, Global Biogeochem. Cy., 12, 35–51, doi:10.1029/97GB02733, 1998.

Hulme, M. and Tosdevin, N.: The Tropical easterly Jet and Sudan rainfall: A review, Theor. Appl. Climatol., 39, 179–187, doi:10.1007/BF00867945, http://dx.doi.org/10.1007/BF00867945, 1989.

Hurrell, J. W., Hack, J. J., Shea, D., Caron, J. M., and Rosinski, J.: A New Sea Surface Temperature and Sea Ice Boundary Dataset for the Community Atmosphere Model, J. Climate, 21, 5145–5153, doi:10.1175/2008JCLI2292.1, http://dx.doi.org/10.1175/2008JCLI2292.1, 2008.

Jenkins, G. S., Gaye, A. T., and Sylla, B.: Late 20th century attribution of drying trends in the Sahel from the Regional Climate Model (RegCM3), Geophys. Res. Let., 32, doi:10.1029/2005GL024225, http://dx.doi.org/10.1029/2005GL024225, l22705, 2005.

Jolly, D., Prentice, I. C., Bonnefille, R., Ballouche, A., Bengo, M., Brenac, P., Buchet, G., Burney, D., Cazet, J.-P., Cheddadi, R., Edorh, T., Elenga, H., Elmoutaki, S., Guiot, J., Laarif, F., Lamb, H., Lezine, A.-M., Maley, J., Mbenza, M., Peyron, O., Reille, M., Reynaud-Farrera, I., Riollet, G., Ritchie, J. C., Roche, E., Scott, L., Ssemmanda, I., Straka, H., Umer, M., Van Campo, E., Vilimumbalo, S., Vincens, A., and Waller, M.: Biome reconstruction from pollen and plant macrofossil data for Africa and the Arabian peninsula at 0 and 6000 years, J. Biogeogr., 25, 1007–1027, doi:10.1046/j.1365-2699.1998.00238.x, 1998.

Joos, F.: Evolution of atmospheric CO_2 over the last 23,000 years, Documentation of CO_2 compilation for PMIP, personal communication, 2016.

Jungclaus, J. H., Fischer, N., Haak, H., Lohmann, K., Marotzke, J., Matei, D., Mikolajewicz, U., Notz, D., and von Storch, J. S.: Characteristics of the ocean simulations in the Max Planck Institute Ocean Model (MPIOM) the ocean component of the MPI-Earth system model, Adv. Mod. Earth Sy., 5, 422–446, doi:10.1002/jame.20023, http://dx.doi.org/10.1002/jame.20023, 2013.

Kattge, J., Díaz, S., Lavorel, S., Prentice, I. C., Leadley, P., et al.: TRY – a global database of plant traits, Glob. Change Biol., 17, 2905–2935, doi:10.1111/j.1365-2486.2011.02451.x, http://dx.doi.org/10.1111/j.1365-2486.2011.02451.x, 2011.

Knorr, W. and Schnitzler, K.-G.: Enhanced albedo feedback in North Africa from possible combined vegetation and soil-formation processes, Clim. Dyn., 26, 55–63, doi:10.1007/s00382-005-0073-9, publisher: Springer, 2006.

Krinner, G., Viovy, N., de Noblet-Ducoudré, N., Ogée, J., Polcher, J., Friedlingstein, P., Ciais, P., Sitch, S., and Prentice, I. C.: A dynamic global vegetation model for studies of the coupled atmosphere-biosphere system, Global Biogeochemical Cycles, 19, n/a–n/a, doi:10.1029/2003GB002199, http://dx.doi.org/10.1029/2003GB002199, gB1015, 2005.

Krinner, G., Lézine, A.-M., Braconnot, P., Sepulchre, P., Ramstein, G., Grenier, C., and Gouttevin, I.: A reassessment of lake and wetland feedbacks on the North African Holocene climate, Geophys. Res. Lett., 39, L07 701, doi:10.1029/2012GL050992, 2012.

Kröpelin, S., Verschuren, D., Lézine, A.-M., Eggermont, H., Cocquyt, C., Francus, P., Cazet, J.-P., Fagot, M., Rumes, B., Russell, J. M., Darius, F., Conley, D. J., Schuster, M., von Suchodoletz, H., and Engstrom, D. R.: Climate-driven ecosystem succession in the Sahara: the past 6000 years, Science, 320, 765–768, doi:10.1126/science.1154913, 2008.

Kutzbach, J. E.: Monsoon climate of the Early Holocene: climate experiment with the Earth's orbital parameters for 9000 years ago, Science, 214, 59–61, doi:10.1126/science.214.4516.59, 1981.

Kutzbach, J. E. and Guetter, P. J.: The influence of changing orbital parameters and surface boundary conditions on climate simulations for the past 18,000 years, J. Atmos. Sci., 43, 1726–1759, 1986.

Kutzbach, J. E. and Liu, Z.: Response of the African monsoon to orbital forcing and ocean feedbacks in the Middle Holocene, Science, 278, 440–443, doi:10.1126/science.278.5337.440, 1997.

Lézine, A.-M.: Timing of vegetation changes at the end of the Holocene humid period in desert areas at the northern edge of the Atlantic and Indian monsoon systems, Comptes Rendus Geoscience, 341, 750–759, doi:10.1016/j.crte.2009.01.001, 2009.

Lézine, A.-M., Hély, C., Grenier, C., Braconnot, P., and Krinner, G.: Sahara and Sahel vulnerability to climate changes, lessons from Holocene hydrological data, Quat. Sc. Rev., 30, 3001–3012, doi:10.1016/j.quascirev.2011.07.006, http://www.sciencedirect.com/science/article/pii/S0277379111002101, 2011a.

Lézine, A.-M., Zheng, W., Braconnot, P., and Krinner, G.: Late Holocene plant and climate evolution at Lake Yoa, northern Chad: pollen data and climate simulations, Clim. Past, 7, 1351–1362, doi:10.5194/cp-7-1351-2011, 2011b.

Liu, Z., Harrison, S. P., Kutzbach, J., and Otto-Bliesner, B.: Global monsoons in the mid-Holocene and oceanic feedback, Climate Dynamics, 22, 157–182, doi:10.1007/s00382-003-0372-y, http://dx.doi.org/10.1007/s00382-003-0372-y, 2004.

Liu, Z., Wang, Y., Gallimore, R., Gasse, F., Johnson, T., deMenocal, P., Adkins, J., Notaro, M., Prentice, I., Kutzbach, J., Jacob, R., Behling, P., Wang, L., and Ong, E.: Simulating the transient evolution and abrupt change of Northern Africa atmosphere-ocean-terrestrial ecosystem in the Holocene, Quaternary Sci. Rev., 26, 1818–1837, doi:10.1016/j.quascirev.2007.03.002, 2007.

McCann, K. S.: The diversity–stability debate, Nature, 405, 228–233, doi:10.1038/35012234, 2000.

Müller, J. M.: Selected climatic data for a global set of standard stations for vegetation science, Junk, The Hague, 1982.

Nicholson, S. E.: The intensity, location and structure of the tropical rainbelt over west Africa as factors in interannual variability, Int. J. Climatol., 28, 1775–1785, doi:10.1002/joc.1507, http://dx.doi.org/10.1002/joc.1507, 2008.

Nicholson, S. E.: The West African Sahel: A Review of Recent Studies on the Rainfall Regime and Its Interannual Variability, ISRN Meteorology, 2013, 1–32, doi:10.1155/2013/453521, 2013.

Nicholson, S. E. and Grist, J. P.: The Seasonal Evolution of the Atmospheric Circulation over West Africa and Equatorial Africa, J. Clim., 16, 1013–1030, doi:10.1175/1520-0442(2003)016<1013:TSEOTA>2.0.CO;2, http://dx.doi.org/10.1175/1520-0442(2003)016<1013:TSEOTA>2.0.CO;2, 2003.

Okumura, Y. and Xie, S.-P.: Interaction of the Atlantic Equatorial Cold Tongue and the African Monsoon, Journal of Climate, 17, 3589–3602, doi:10.1175/1520-0442(2004)017<3589:IOTAEC>2.0.CO;2, https://doi.org/10.1175/1520-0442(2004)017<3589:IOTAEC>2.0.CO;2, 2004.

Otto, J., Raddatz, T., and Claussen, M.: Strength of forest-albedo feedback in mid-Holocene climate simulations, Clim. Past, 7, 1027–1039, doi:10.5194/cp-7-1027-2011, http://www.clim-past.net/7/1027/2011/, 2011.

Pausata, F., Messori, G., and Zhang, Q.: Impacts of dust reduction on the northward expansion of the African monsoon during the Green Sahara period, EPSL, 434, 298–307, doi:10.1016/j.epsl.2015.11.049, http://www.sciencedirect.com/science/article/pii/S0012821X15007530, 2016.

Pavlick, R.: Development and evaluation of a diverse dynamic global vegetation model based on plant functional tradeoffs, Ph.D. thesis, Universität Hamburg, 2012.

Prentice, I., Cramer, W., Harrison, S., Leemans, R., Monserud, R., and Solomon, A.: Special Paper: A Global Biome Model Based on Plant Physiology and Dominance, Soil Properties and Climate, J. Biogeogr., 19, 117–134, doi:10.2307/2845499, 1992.

Rachmayani, R., Prange, M., and Schulz, M.: North African vegetation-precipitation feedback in early and mid-Holocene climate simulations with CCSM3-DGVM, Clim. Past, 11, 175–185, doi:10.5194/cp-11-175-2015, 2015.

Raddatz, T. J., Reick, C. H., Knorr, W., Kattge, J., Roeckner, E., Schnur, R., Schnitzler, K.-G., Wetzel, P., and Jungclaus, J.: Will the tropical land biosphere dominate the climate - carbon cycle feedback during the twenty-first century?, Clim. Dynam., 29, 565–574, doi:10.1007/s00382-007-0247-8, 2007.

Reick, C. H., Raddatz, T., Brovkin, V., and Gayler, V.: Representation of natural and anthropogenic land cover change in MPI-ESM, Adv. Model. Earth Sy., 5, 459–482, doi:10.1002/jame.20022, 2013.

Ritchie, J. and Haynes, C.: Holocene vegetation zonation in the eastern Sahara, Nature, 330, 645–647, doi:10.1038/330645a0, 1987.

Scheiter, S., Langan, L., and Higgins, S. I.: Next-generation dynamic global vegetation models: learning from community ecology, New Phytol., 198, 957–969, doi:10.1111/nph.12210, 2013.

Scherer-Lorenzen, M.: Biodiversity and ecosystem functioning: basic principles, in: Biodiversity: Structure and Function. In Encyclopedia of Life Support Systems (EOLSS) vol Developed under the Auspices of the UNESCO, edited by Barthlott, W., Linsenmair, K. E., and Porembski, S., EOLSS Publisher, Oxford, 2005.

Schlesinger, W. H., Reynolds, J. F., Cunningham, G. L., Huenneke, L. F., Jarrell, W. M., Virginia, R. A., and Whitford, W. G.: Biological feedbacks in global desertification, Science, 247, 1043–1048, doi:10.1126/science.247.4946.1043, 1990.

Schlesinger, W. H., Raikes, J. A., Hartley, A. E., and Cross, A. F.: On the Spatial Pattern of Soil Nutrients in Desert Ecosystems, Ecology, 77, 364–374, doi:10.2307/2265615, http://dx.doi.org/10.2307/2265615, 1996.

Shanahan, T. M., Mckay, N. P., Hughen, K. A., Overpeck, J. T., Otto-Bliesner, B., Heil, C. W., King, J., Scholz, C. A., and Peck, J.: The time-transgressive termination of the African humid period, Nat. Geosc., 8, 140–144, doi:10.1038/ngeo2329, 2015.

Smith, B., Prentice, I. C., and Sykes, M. T.: Representation of vegetation dynamics in the modelling of terrestrial ecosystems: comparing two contrasting approaches within European climate space, Glob. Ecol. Biogeogr., 10, 621–637, 2001.

Stevens, B., Giorgetta, M., Esch, M., Mauritsen, T., Crueger, T., Rast, S., Salzmann, M., Schmidt, H., Bader, J., Block, K., Brokopf, R., Fast, I., Kinne, S., Kornblueh, L., Lohmann, U., Pincus, R., Reichler, T., and Roeckner, E.: Atmospheric component of the MPI-M Earth System Model: ECHAM6, Adv. Mod. Earth Sys., 5, 146–172, doi:10.1002/jame.20015, http://dx.doi.org/10.1002/jame.20015, 2013.

Texier, D., de Noblet, N., Harrison, S. P., Haxeltine, A., Jolly, D., Joussaume, S., Laarif, F., Prentice, I. C., and Tarasov, P.: Quantifying the role of biosphere-atmosphere feedbacks in climate change: coupled model simulations for 6000 years BP and comparison with palaeodata for northern Eurasia and northern Africa, Clim. Dynam., 13, 865–882, doi:10.1007/s003820050202, 1997.

Texier, D., de Noblet, N., and Braconnot, P.: Sensitivity of the African and Asian Monsoons to Mid-Holocene Insolation and Data-Inferred Surface Changes, J. Clim., 13, 164–181, doi:10.1175/1520-0442(2000)013<0164:SOTAAA>2.0.CO;2, http://dx.doi.org/10.1175/1520-0442(2000)013<0164:SOTAAA>2.0.CO;2, 2000.

Vamborg, F. S. E., Brovkin, V., and Claussen, M.: The effect of a dynamic background albedo scheme on Sahel/Sahara precipitation during the mid-Holocene, Clim. Past, 7, 117–131, doi:10.5194/cp-7-117-2011, 2011.

Van Bodegom, P. M., Douma, J. C., Witte, J. P. M., Ordonez, J. C., Bartholomeus, R. P., and Aerts, R.: Going beyond limitations of plant functional types when predicting global ecosystem–atmosphere fluxes: exploring the merits of traits-based approaches, Glob. Ecol. Biogeogr., 21, 625–636, doi:10.1111/j.1466-8238.2011.00717.x, http://dx.doi.org/10.1111/j.1466-8238.2011.00717.x, 2012.

Vellend, M., Verheyen, K., Jacquemyn, H., Kolb, A., Van Calster, H., Peterken, G., and Hermy, M.: Extinction debt of forest plants persists for more than a century following habitat fragmentation, Ecology, 87, 542–548, doi:10.1890/05-1182, 2006.

Verheijen, L., Aerts, R., Brovkin, V., Cavender-Bares, J., Cornelissen, J., Kattge, J., and van Bodegom, M.: Inclusion of ecologically based trait variation in plant functional types reduces the projected land carbon sink in an earth system model, Glob. Change Biol., 21, 3074–3086, doi:10.1111/gcb.12871, 2015.

Verheijen, L. M., Brovkin, V., Aerts, R., Bönisch, G., Cornelissen, J. H. C., Kattge, J., Reich, P., Wright, I., and van Bodegom, P.: Impacts of trait variation through observed trait–climate relationships on performance of an Earth system model: a conceptual analysis, Biogeosciences, 10, 5497–5515, doi:10.5194/bg-10-5497-2013, 2013.

Wang, H., Prentice, I. C., Keenan, T. F., Davis, T. W., Wright, I. J., Cornwell, W. K., Evans, B. J., and Peng, C.: Towards a universal model for carbon dioxide uptake by plants, Nature Plants, 3, 734–741, doi:https://doi.org/10.1038/s41477-017-0006-8, 2017.

Watrin, J., Lézine, A.-M., Hély, C., Cour, P., Ballouche, D., and Contributors: Plant migration and plant communities at the time of the “Green Sahara”, histoire climatique des déserts d’Afrique et d’Arabie Climatic history of the African and Arabian deserts, CR Geosci., 341, 656–670, doi:10.1016/j.crte.2009.06.007, 2009.

Whitford, W.: Ecology of Desert Systems, Elsevier Science, https://books.google.de/books?id=OZ4hZbXS8IcC, 2002.

Williams, J. W., Blois, J. L., and Shuman, B. N.: Extrinsic and intrinsic forcing of abrupt ecological change: case studies from the late Quaternary, J. Ecol., 99, 664–677, doi:10.1111/j.1365-2745.2011.01810.x, 2011.

Wullschleger, S. D., Epstein, H. E., Box, E. O., Euskirchen, E. S., Goswami, S., Iversen, C. M., Kattge, J., Norby, R. J., van Bodegom, P. M., and Xu, X.: Plant functional types in Earth system models: past experiences and future directions for application of dynamic vegetation models in high-latitude ecosystems, Annals of Botany, 114, 1–16, doi:10.1093/aob/mcu077, +http://dx.doi.org/10.1093/aob/mcu077, 2014.